
ELSEVIER
Volume 30 Issues 7–8 April 2011 ISSN 0277-3791
QUATERNARY
SCIENCE REVIEWS
The International Multidisciplinary Research and Review Journal
Editor-in-Chief
C.V. Murray-Wallace
Editorial Team
H. Bauch
J. Carrión
N. Glasser
C. Hillaire-Marcel
C.N. Roberts
X. Yang

Quaternary Science Reviews 30 (2011) 947–966

Contents lists available at ScienceDirect

Quaternary Science Reviews

journal homepage: www.elsevier.com/locate/quascirev

Modern pollen distributions in Qinghai-Tibetan Plateau and the development of transfer functions for reconstructing Holocene environmental changes

Houyuan Lu [a,*], Naiqin Wu [a], Kam-biu Liu [b], Liping Zhu [c], Xiangdong Yang [d], Tandong Yao [c], Luo Wang [a], Quan Li [a], Xingqi Liu [d], Caiming Shen [e], Xiaoqiang Li [f], Guobang Tong [g], Hui Jiang [h]

[a] Key Laboratory of Cenozoic Geology and Environment, Institute of Geology and Geophysics, Chinese Academy of Sciences, Beijing 100029, China
[b] Department of Oceanography and Coastal Sciences, Louisiana State University, Baton Rouge, LA 70803, USA
[c] Institute of Tibetan Plateau Research, Chinese Academy of Sciences, Beijing 100085, China
[d] State Key Laboratory of Lake Science and Environment, Nanjing Institute of Limnology and Geography, Chinese Academy of Sciences, Nanjing 210008, China
[e] Atmospheric Sciences Research Center, State University of New York, Albany, NY 12203, USA
[f] Institute of Vertebrate Paleontology and Paleoanthropology, Chinese Academy of Sciences, Beijing 100044, China
[g] Institute of Hydrology and Geology, Chinese Academy of Geological Sciences, Zhengding 050803, China
[h] State Key Laboratory of Estuarine and Coastal Research, East China Normal University, Shanghai 200062, China

A R T I C L E I N F O

Article history:
Received 23 March 2010
Received in revised form
23 December 2010
Accepted 18 January 2011
Available online 9 February 2011

Keywords:
Qinghai-Tibetan plateau
Vegetation
Pollen
Transfer functions
Holocene
Climatic changes

A B S T R A C T

This study investigates the distribution of modern pollen assemblages in the Qinghai-Tibetan Plateau, China, based on surface soil samples collected at 1202 sites along an altitudinal gradient of 10–5500 m asl, where mean annual precipitation (MAP) ranges from 12 to 1840 mm and mean annual temperature (MAT) from −7 to 21.5 °C. A total of 153 pollen taxa were found with relative abundances greater than 1% in at least two samples. Canonical correspondence analysis (CCA) was used to determine the main environmental variables influencing pollen distributions. The results reveal that MAP is the most significant dominant variable. However, MAT, altitude (ALT), July temperature (MT7), and relative humidity (HHH) are also significant variables that clearly follow the gradients in the CCA ordination, suggesting that pollen assemblages probably not only reflect a single climatic parameter, but also a variety of other climatic inter-related parameters.

Transfer functions, based on locally weighted weighted averaging (LWWA), were developed for MAP (R^2-boot = 0.89, RMSEP = 109 mm), MAT (R^2-boot = 0.78, RMSEP = 2.3 °C), ALT (R^2-boot = 0.73, RMSEP = 597 m), HHH (R^2-boot = 0.82, RMSEP = 4.5%), and July mean precipitation (MP7) (R^2-boot = 0.87, RMSEP = 23 mm). Overall, our results confirm that pollen can provide reliable estimates of the primary climatic parameters. The application of the LWWA model to the fossil records of Chen Co Lake allowed quantitative inferences to be made about Holocene climatic changes in the southern Tibetan Plateau, suggesting that LWWA is a robust calibration method for quantitative palaeo-environmental reconstruction based on pollen data in the regions.

1. Introduction

Accurate quantitative reconstructions of regional environmental patterns are needed to understand the global and regional changes in climate and environment and to assess global circulation models on a regional scale (COHMAP Members, 1988; Holmgren and Tjus, 1996; Nakagawa et al., 2002; Seppä et al., 2004; Lu et al., 2007). The Qinghai-Tibetan Plateau, with an area of over 2.3 million km^2 at an average elevation of over 4000 m asl, is the largest and highest mountain plateau on Earth (Liu and Chen, 2000). Its global significance does not lie simply in its physical parameters, but more importantly in influencing the atmospheric circulation of the Northern Hemisphere, and in constituting a significant forcing factor on the intensity of the Asian monsoons (Kutzbach et al., 1989; An et al., 2001). However, there are only a few quantitative environmental records available for the Qinghai-Tibetan Plateau region (Shen, 2006,2008; Herzschuh et al., 2009a,b,2010). These are generally limited to tree ring studies (Shao et al., 2005; Gou et al., 2007), ice core records (Yao et al., 2008), and meteorological records (the latter spanning less than 40 years).

Recent advances in quantitative environmental reconstruction techniques have led to rapid expansion of fossil-based long-term

* Corresponding author. Tel.: +86 10 82998259; fax: +86 10 8299 8122.
E-mail address: Houyuanlu@mail.iggcas.ac.cn (H. Lu).

0277-3791/$ – see front matter © 2011 Elsevier Ltd. All rights reserved.
doi:10.1016/j.quascirev.2011.01.008

quantitative palaeo-environmental reconstructions. Such investigations are usually based on mathematical transfer functions that transform fossil assemblages into quantitative estimates of past environmental conditions (Imbrie and Kipp, 1971; Liu and Lam, 1985; Overpeck et al., 1985; Guiot et al., 1989; ter Braak and Juggins, 1993; Birks, 1995, 2003; Gasse et al., 1995; Nakagawa et al., 2002; Yang et al., 2003; Seppä et al., 2004; Lu et al., 2006; Zhang et al., 2007; Bjune et al., 2009; Seppä et al., 2009; Jiang et al., 2010). Among the numerous fossil indicators, sedimentary pollen records have been emerging as a promising source of information to quantify past environmental changes in several regions of the globe, including Africa (Gajewski et al., 2002), Europe (Guiot, 1990; Guiot et al., 1993; Seppä et al., 2004), Northern America (Whitmore et al., 2005; Brown et al., 2006), Japan (Nakagawa et al., 2002), Australia (Cook and Kaars, 2006), Russia (Tarasov et al., 2005; Solovieva et al., 2005), and China (Song et al., 1997; Shen (2006); Li et al., 2007; Jiang et al., 2010).

Quantitative inferences based on pollen rely on transfer functions from surface sediment samples analyzed along broad environmental gradients. A strong numerical relationship between modern pollen and environmental variables of interest is required to develop reliable transfer functions (Birks, 1998). During the past decade, modern surface pollen studies have been published for many parts of China (Huang et al., 1993; Wu and Xiao, 1995; Sun et al., 1996; Song et al., 1997; Cour et al., 1999; Liu et al., 1999; Members of China Quaternary Pollen Data Base, 2001; Yu et al., 2001; Yan et al., 2004; Zheng et al., 2008; Lu et al., 2008; Zhao and Herzschuh, 2009; Zhao et al., 2009). In the Qinghai-Tibetan Plateau, for example, Yu et al. (2001) successfully used modern pollen datasets to study the relationships between modern pollen rain and vegetation based on 316 surface samples. However, the datasets were mostly obtained from the eastern side of the Qinghai-Tibetan Plateau. Furthermore, pollen-climate inference models have not been developed or used to reconstruct past climatic changes in this region based on 316 surface samples (Yu et al., 2001).

Recently, Shen (2006) and Herzschuh et al. (2009a,b, 2010) used pollen to reconstruct changes in temperature and precipitation based on 227 surface soil samples and 112 lake surface sediments from the eastern Qinghai-Tibetan Plateau, respectively. However, only 20 pollen types were selected to represent all of pollen types in the modern pollen spectra (Shen, 2006). Furthermore, the pollen percentages used in the calibration model were recalculated based on a sum of 20 pollen types (Shen, 2006).

Herzschuh et al. (2010) have successfully established the quantitative relationships between modern pollen rain and climate parameters, and reconstructed palaeo-climatic changes on the basis of 112 lake surface samples in eastern regions of the Qinghai-Tibetan Plateau. However, the use of more modern pollen assemblages from wider range of climatic-geographical zones to quantitatively reconstruct more environmental variables in addition to temperature and precipitation has not been explored, because the distribution optima of individual pollen taxa with respect to environmental factors have been poorly documented in broad areas of the Qinghai-Tibetan Plateau.

Here we used a large modern pollen dataset consisting of 1202 modern surface samples along significant ecological and climatic gradients over the Qinghai-Tibetan (Xizang) Plateau and Xinjiang, China, to develop transfer functions for quantitative reconstruction of palaeo-environments. Our research aims are: (1) to discuss the relationships between pollen assemblages from surface sediments and modern environmental variables, such as mean annual precipitation (MAP), mean annual temperature (MAT), and relative humidity (HHH), among others; (2) to determine the environmental variables that are most likely to be responsible for controlling the spatial distribution of pollen and therefore most useful in the derivation of climatic transfer functions; (3) to derive a set of pollen-environment transfer functions for the quantitative reconstruction of palaeo-climate and palaeo-environment in the Qinghai-Tibetan Plateau; and (4) lastly, a case study was conducted to quantitatively reconstruct the Holocene climatic changes based on a fossil pollen record from Chen Co Lake in the southern Tibetan Plateau, and to illustrate the applicability of transfer functions to subalpine palaeo-climatic reconstruction.

2. Study area

2.1. Climate

The study area is located between latitudes of 21°–48° N and longitudes of 74°–109° E at an altitudinal range between ca.10 and 5500 m asl (above sea level) (Fig. 1). Some samples were taken from neighboring areas to the north and south of the Qinghai-Tibetan Plateau at lower elevation (<100 m). Some samples were collected along the alpine altitudinal climatic gradients from tropical-subtropical at the base of the mountains to permanent ice and snow at the highest elevations, including the Gongga Mountains at elevations of 1000–4500 m asl in the east (Fig. 2), and the Himalayan mountains at elevations of 100–5200 m asl in the south (Fig. 1).

The Plateau has very steep climatic and environmental gradients (from north to south, and from west to east), which span several climate zones from the extremely arid zone of middle temperate in the north to the alpine sub-frigid zone in the central part, to the alpine temperate zone in the south, and the subtropical zone in the southeast. The major part of the Qinghai-Tibetan Plateau higher than 4500 m asl is characterized by cold-dry winters and cool-humid summers with mean annual temperature (MAT) of −7–8 °C (Fig. 3A). Extremely dry conditions occur in the northern margin, having a mean annual precipitation (MAP) of about 10–30 mm. The southern and southeastern Plateau has relatively high rainfall, with MAP ranging from 370 mm to over 1800 mm (Fig. 3B).

2.2. Vegetation

Vegetation distribution in the Qinghai-Tibetan Plateau is largely controlled by summer monsoon rainfalls coming from the

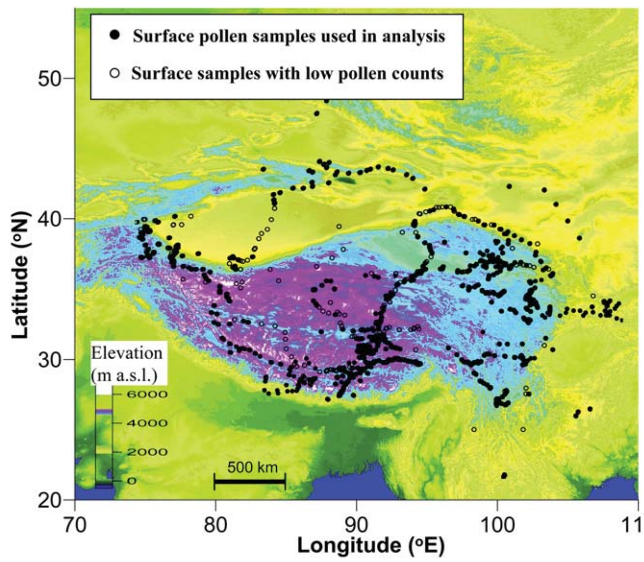

Fig. 1. Topographic map of the Qinghai-Tibetan Plateau showing sites of modern pollen samples.

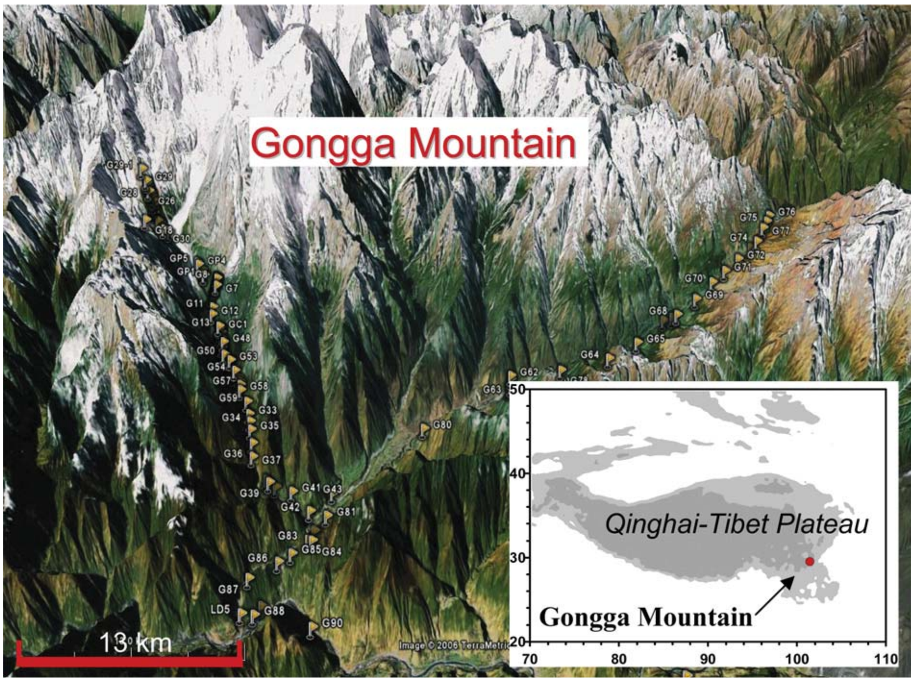

Fig. 2. Remote sensing map of the Gongga Mountain (after Googles Earth) located on the eastern part of the Qinghai-Tibetan Plateau (inset). Fanion symbol indicates the sites of modern pollen samples.

southeast. It is characterized by a zonal pattern from the southeast to northwest following a gradient of decreasing moisture (precipitation), ranging from I Forest, II Scrub, III Steppe, IV Alpine meadow, V Desert steppe to VI Desert and alpine desert (ITCAS, 1988; Institute of Geography, 1990, 1999) (Fig. 4).

Coniferous and broadleaved forests, consisting mainly of *Picea, Abies, Pinus, Tsuga, Betula, Populus,* and *Quercus*, grow in valleys and mountain slopes below 4000 m. Subalpine dark coniferous forests are mainly distributed in the northern slopes of some mountains at an elevation of about 3100–3500 m in the southeast, 3500–4100 m in the west, and 2800–3800 m in the northwest. Scrubs, generally including evergreen sclerophyllous, evergreen coniferous, deciduous broadleaved, and succulent plants, are distributed at different elevations of the Plateau. Alpine meadow occupies the eastern part of the Plateau over 4000 m in altitude. It consists mainly of sedge and grass communities such as *Carex, Kobresia, Stipa, Festuca, Poa, Roegneria,* and *Koeleria*, together with some species of Composite, Chenopodiaceae, Ranunculaceae, Polygonaceae, and Leguminosae.

Alpine steppes occupy a vast region at elevations of 4400–5400 m in the interior of the Plateau. *Stipa purpurea, S. basiplumosa, Carex moorcroftii* and *Artemisia wellbyi* are dominants of steppes. Usually there are some cushion plants (e.g. *Arenaria musciformis, Androsace tapete*) and succulent plants (CAM plants: *Rhodiola* spp.; *Sedum* spp.) (Chang, 1981; ITCAS, 1988; Wang, 1988). Alpine desert is found in the western part of the Tibetan Plateau, where the elevation of the plateau surface and lake basins is over 4500 m. The dominants of this vegetation type are cushion minor semi-scrubs adapted to an extremely cold and dry climate. The representative community is composed of *Ceratoides compacta*, *Rhodiola* spp., and *Sedum* spp. Companion species are high mountain plants including *Ajania trilobata, Arenaria monticola, Carex moorcroftii, Hedinia tibetica, Oxytropis densa, Pegaeophyton scapiflorum, Stipa basiplumosa* and *Thylacospemum caespitosum* (Chang, 1981; Wang, 1988; ITCAS, 1988; Institute of Geography, 1990, 1999).

3. Materials and methods

3.1. Pollen sample collection and analysis

A total of 1320 surface samples were initially used for this study (Fig. 1), including 185 surface samples derived from the Chinese Quaternary Pollen Data Base (Members of China Quaternary Pollen Database, 2001). Subsequently 118 of the new samples were excluded because these samples were taken from deserts or the extreme arid-cold region and hence containing few pollen grains (Fig. 1). Thus, a total of 1202 surface samples were used in this study.

Pollen samples used in this study were collected from a variety of vegetation types. Two or three subsamples within an area of ca. 30 m^2 were mixed into one sample at each site (excluding 137 lake surface samples). Their geographic locations were determined using GPS. Altitude was determined using a Pocket-Altimeter Barometer, which was calibrated at the locations of known altitude during the course of each day. Diurnal pressure variations cause an error of approximately ± 30 m in absolute altitude determination. The new 1135 (excluding 185 samples from Chinese Quaternary Pollen Database) samples were taken from topsoil, lake surface sediments, and moss polster from 1998 to 2009 A.D.

Samples were mostly prepared using standard techniques outlined in Fægri and Iversen (1975), involving alkali digestion, treatment with 10% cold HCl, 10% hot KOH, 46% hot HF, and Erdtman's acetolysis, staining with safranin, dehydration with tertiary butyl alcohol, and mounting in silicone oil. Prior to alkali digestion, moss polsters and soils were dispersed in distilled water and sieved (200 μm) to remove coarse detritus and sand. A Leica microscope at a magnification of 400× was used for pollen identification and counting. More than 300 pollen grains were counted for each sample. Pollen abundance was expressed as percentages calculated using the total pollen sum.

Pollen identification was aided by the use of a modern pollen reference collection and published keys (South China Institute of

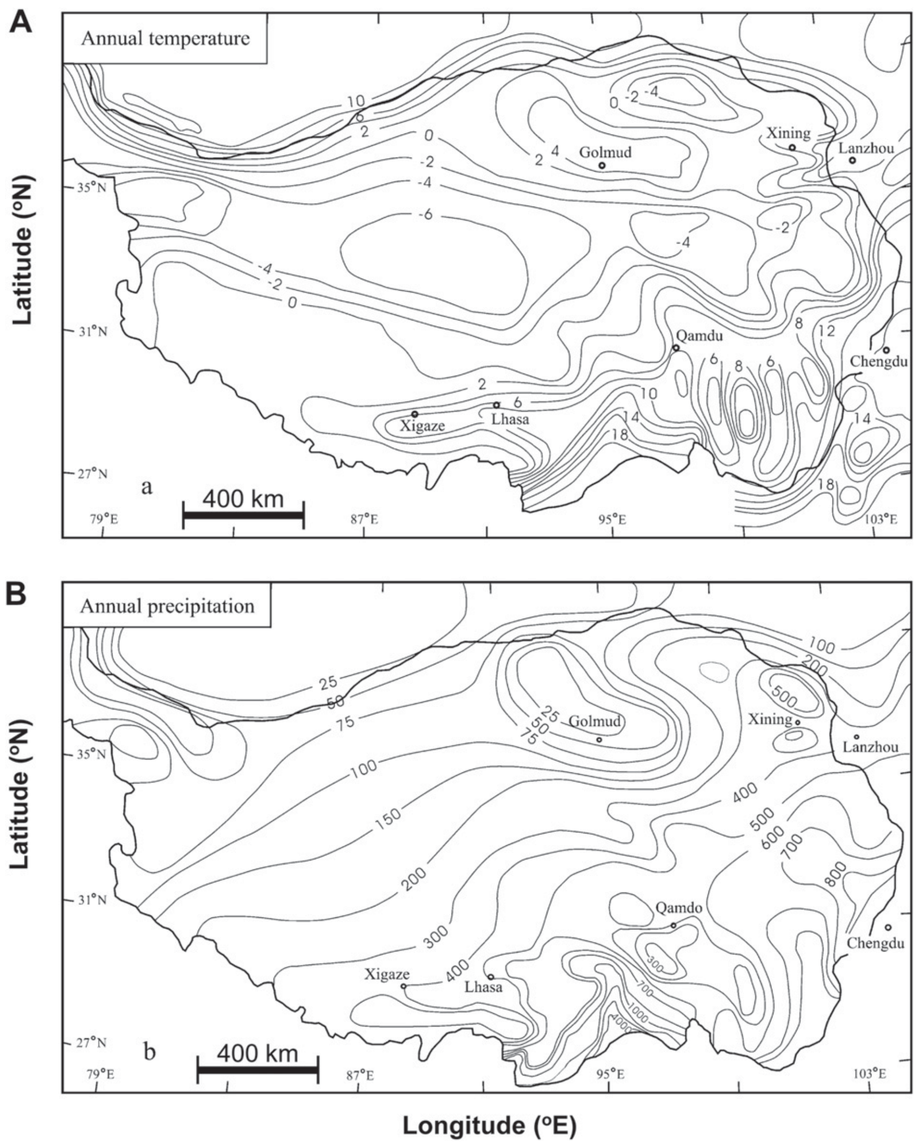

Fig. 3. Isotherm and isohyet map for the Qinghai-Tibetan Plateau. A. Mean annual temperature (°C). B. Mean annual precipitation (mm) in the Qinghai-Tibetan Plateau (modified from Institute of Geography, Chinese Academy of Science, 1990).

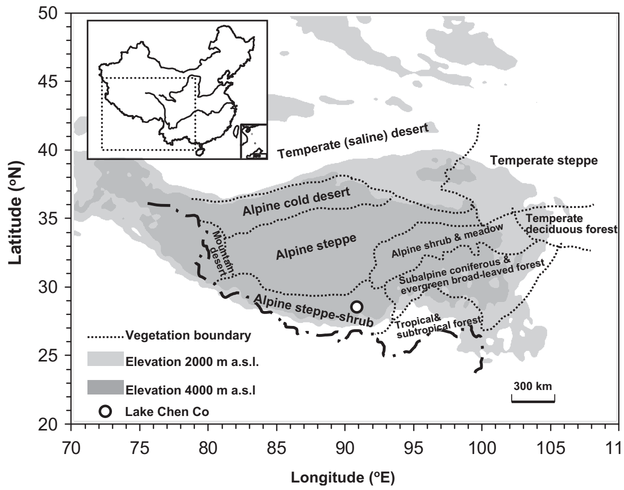

Fig. 4. Map of the Qinghai-Tibetan Plateau showing regional vegetation. (The vegetation zonations modified from Institute of Geography, Chinese Academy of Science, 1990, 1999).

Botany & Institute of BotanyAcademia Sinica, 1982; Zhang et al., 1990; Wang et al., 1995). A total of 214 pollen taxa and other unidentified taxa were recognized from the surface-sediment samples of the 1202 study sites (Table 1). The percentage of pollen data were square root transformed prior to numerical analyses in order to stabilize their variances. All pollen taxa with relative abundances of >1% in at least two samples were used in data analyses.

3.2. Environmental parameters collection

Modern climatic data for spatial interpolation (Lin et al., 2002) were derived from a database consisting of 996 meteorological stations, including 733 meteorological stations from China Meteorological Administration (CMA) and 263 meteorological stations from http://www.ncdc.noaa.gov/oa/ncdc.html, covering the areas surrounding the Qinghai-Tibetan Plateau, including India, Nepal, Pakistan, Afghanistan, Kazakhstan, Kirghizia, and Mongolia. For most meteorological stations, the length of record exceeds 30 years. Fourteen environmental variables were chosen: altitude (ALT),

Table 1
List of the 215 pollen taxa retained in the modern database, derived from 1202 sites of surface soil sediments.

No.	Pollen Taxa	Taxa code	N[a]	Hill's N2[a]	Minimum	Maximum	Mean	Standard deviation
1	*Abies*	ABIE	299	52.9	0.0	72.2	0.8	4.0
2	*Picea*	PICE	568	121.9	0.0	69.0	2.5	7.8
3	*Pinus*	PINU	1122	465.4	0.0	98.4	19.3	25.9
4	*Tsuga*	TSUG	432	166.6	0.0	14.3	0.5	1.3
5	*Larix*	LARI	115	10.2	0.0	57.5	0.2	2.3
6	*Ketelleria*	KETE	11	3.1	0.0	4.2	0.0	0.1
7	*Cedrus*	CEDR	9	6.3	0.0	0.9	0.0	0.0
8	Taxodiaceae	TAXO	25	9.6	0.0	5.3	0.0	0.2
9	Cupressaceae	CUPR	317	34.0	0.0	75.2	0.5	3.3
10	*Sabina*	SABI	7	3.8	0.0	2.4	0.0	0.1
11	*Ephedra*	EPHE	535	89.8	0.0	85.1	1.7	6.3
12	*Betula*	BETU	695	173.3	0.0	51.2	1.7	4.4
13	*Alnus*	ALNU	367	84.8	0.0	28.9	0.4	1.5
14	*Corylus*	CORY	326	114.0	0.0	16.0	0.5	1.7
15	*Carpinus*	CARP	181	43.4	0.0	25.7	0.3	1.5
16	*Pterocarya*	PTCA	9	5.5	0.0	1.1	0.0	0.0
17	*Tilia*	TILI	11	7.9	0.0	0.6	0.0	0.0
18	*Ulmus*	ULMU	167	65.2	0.0	5.0	0.1	0.3
19	*Celtis*	CELT	13	8.9	0.0	0.7	0.0	0.0
20	*Salix*	SALI	365	50.4	0.0	60.8	0.6	3.0
21	*Juglans*	JUGL	274	92.6	0.0	11.4	0.2	0.7
22	*Castanea*	CAST	87	6.2	0.0	54.8	0.1	2.1
23	*Carya*	CARY	12	9.2	0.0	0.8	0.0	0.0
24	*Quercus-deciduous*	QUDE	381	70.7	0.0	67.3	1.3	5.4
25	*Quercus– evergreen*	QUGR	150	30.5	0.0	49.0	0.4	2.6
26	*Castanopsis*	CASN	63	5.7	0.0	37.1	0.1	1.1
27	*Fagus*	FAGU	7	3.6	0.0	1.3	0.0	0.0
28	*Cyclobalanopsis*	CYCL	19	4.5	0.0	23.5	0.1	0.9
29	*Populus*	POPU	33	17.9	0.0	3.0	0.0	0.2
30	*Melia*	MELI	1	1.0	0.0	1.7	0.0	0.0
31	*Myricaria*	MYRI	80	19.2	0.0	28.6	0.2	1.5
32	*Tamarix*	TAMA	132	29.3	0.0	29.0	0.2	1.5
33	*Reaumuria*	REAU	20	6.3	0.0	22.1	0.1	0.8
34	Ericaceae	ERIC	247	36.9	0.0	80.6	0.9	5.4
35	*Fraxinus*	FRAX	56	23.3	0.0	2.8	0.0	0.1
36	*Rhamnus*	RHAM	69	37.0	0.0	4.2	0.1	0.3
37	*Ilex*	ILEX	19	9.1	0.0	2.2	0.0	0.1
38	Oleaceae	OLEA	63	33.2	0.0	2.8	0.0	0.2
39	*Ligustrum*	LIGU	23	3.8	0.0	18.1	0.0	0.6
40	*Acer*	ACER	70	35.1	0.0	2.4	0.0	0.1
41	Euphorbiaceae	EUPH	164	27.0	0.0	15.8	0.1	0.8
42	Loranthaceae	LORA	4	1.7	0.0	3.5	0.0	0.1
43	*Loropetalum*	LORO	1	1.0	0.0	0.2	0.0	0.0
44	*Rhus*	RHUS	31	15.8	0.0	2.9	0.0	0.2
45	*Nyssa*	NYSS	1	1.0	0.0	2.2	0.0	0.1
46	*Acanthopanax*	ACAN	41	15.6	0.0	2.4	0.0	0.1
47	Acanthaceae	ACAE	17	3.5	0.0	5.2	0.0	0.1
48	*Nerium*	NERI	7	3.2	0.0	5.6	0.0	0.2
49	Myrtaceae	MYRT	10	8.6	0.0	0.6	0.0	0.0
50	*Morus*	MORU	49	11.0	0.0	8.8	0.0	0.3
51	*Microtropis*	MICR	21	14.3	0.0	1.0	0.0	0.0
52	Rutaceae	RUTA	44	20.7	0.0	3.3	0.0	0.1
53	*Sambucus*	SAMB	90	37.5	0.0	3.9	0.0	0.2
54	Thymelaeaceae	THYM	25	16.5	0.0	1.1	0.0	0.1
55	*Stellera*	STEL	37	4.5	0.0	49.6	0.1	1.4
56	*Berberis*	BERB	23	8.9	0.0	3.4	0.0	0.1
57	*Dipsacus*	DIPS	26	8.0	0.0	4.5	0.0	0.2
58	*Elaeagnus*	ELAG	75	10.2	0.0	17.9	0.1	0.6
59	Caprifoliaceae	CAPR	65	18.1	0.0	5.2	0.0	0.3
60	*Caragana*	CARA	101	43.1	0.0	6.5	0.1	0.4
61	*Alhagi*	ALHA	11	1.9	0.0	6.7	0.0	0.2
62	*Astragalus*	ASTR	29	3.5	0.0	26.5	0.0	0.8
63	Leguminosae	LEGU	531	210.3	0.0	14.5	0.6	1.5
64	*Hippophae*	HIPP	89	32.1	0.0	6.7	0.1	0.4
65	*Apocynum*	APOC	2	1.1	0.0	8.9	0.0	0.2
66	Calligonum	CALL	15	8.8	0.0	1.0	0.0	0.0
67	*Nitraria*	NITR	313	41.3	0.0	98.9	1.0	5.7
68	*Tribulus*	TRIB	87	31.8	0.0	20.1	0.2	1.3
69	*Arenaria*	AREN	239	39.4	0.0	88.9	0.9	5.0
70	Caryophyllaceae	CARL	302	66.8	0.0	36.7	0.4	1.7
71	*Rhodiola*	RHDL	274	94.6	0.0	15.2	0.3	1.1
72	Solanaceae	SOLA	180	49.3	0.0	14.4	0.2	0.8
73	Ranunculaceae	RANU	689	245.6	0.0	29.3	1.1	2.2

(*continued on next page*)

Table 1 (*continued*)

No.	Pollen Taxa	Taxa code	N[a]	Hill's N2[a]	Minimum	Maximum	Mean	Standard deviation
74	Labiate	LABI	449	99.5	0.0	55.0	0.8	2.7
75	*Arisaema*	ARIS	12	3.2	0.0	5.9	0.0	0.2
76	*Cannabis*	CANN	6	4.3	0.0	1.1	0.0	0.0
77	Celastraceae	CELA	5	2.6	0.0	1.0	0.0	0.0
78	Convolulaceae	CONV	148	66.9	0.0	4.7	0.1	0.3
79	*Cornus*	CORN	20	14.0	0.0	0.5	0.0	0.0
80	*Frankenia*	FRAN	2	2.0	0.0	1.0	0.0	0.0
81	*Gentiana*	GENT	107	28.3	0.0	8.1	0.1	0.4
82	*Geranium*	GERA	48	4.2	0.0	35.8	0.1	1.3
83	Gesneriaceae	GESN	50	27.6	0.0	2.6	0.0	0.1
84	*Impatiens*	IMPA	35	10.3	0.0	5.9	0.0	0.2
85	*Lythrum*	LYTH	4	3.1	0.0	0.6	0.0	0.0
86	*Monotropa*	MONO	2	1.9	0.0	0.2	0.0	0.0
87	Malvaceae	MALV	7	6.2	0.0	0.3	0.0	0.0
88	*Papaver*	PAPA	38	15.1	0.0	2.4	0.0	0.1
89	*Veronica*	VERO	81	17.6	0.0	32.0	0.2	1.4
90	Scrophulariaceae	SCRO	232	38.1	0.0	28.8	0.2	1.1
91	*Androsace*	ANDR	74	24.1	0.0	7.3	0.1	0.4
92	*Primula*	PRIM	187	69.5	0.0	5.8	0.1	0.5
93	Rubiaceae	RUBI	31	6.6	0.0	6.1	0.0	0.2
94	Rosaceae	ROSA	732	284.1	0.0	29.4	1.8	3.4
95	*Spiraea*	SPIR	292	94.9	0.0	15.4	0.2	0.8
96	*Potentilla*	POTE	216	56.7	0.0	22.2	0.2	1.0
97	*Filipendula*	FILI	59	40.6	0.0	2.6	0.0	0.2
98	Gramineae	GRAM	1061	338.9	0.0	91.0	4.8	8.1
99	Chenopodiaceae	CHEN	988	312.9	0.0	100.0	11.0	19.6
100	*Artemisia*	ARTE	1188	520.1	0.0	97.8	16.5	20.3
101	Composite	COMP	1042	353.5	0.0	52.8	2.8	4.6
102	*Plantago*	PLAN	117	43.4	0.0	10.7	0.1	0.7
103	Polemoniaceae	POLE	47	15.7	0.0	6.0	0.0	0.3
104	*Humulus*	HUMU	119	29.2	0.0	9.8	0.1	0.4
105	*Pyrola*	PYRO	17	8.2	0.0	1.9	0.0	0.1
106	*Orostachys*	OROS	2	1.4	0.0	1.0	0.0	0.0
107	*Plumbago*	PLUM	2	1.8	0.0	0.8	0.0	0.0
108	*Polygala*	POLY	1	1.0	0.0	1.0	0.0	0.0
109	*Urtica*	URTI	54	4.7	0.0	20.3	0.0	0.8
110	Valerianaceae	VALE	13	5.4	0.0	2.3	0.0	0.1
111	Verbenaceae	VERB	11	3.7	0.0	2.5	0.0	0.1
112	*Passiflora*	PASS	1	1.0	0.0	0.4	0.0	0.0
113	*Viola*	VIOL	71	19.4	0.0	5.4	0.0	0.3
114	*Wikstroemia*	WIKS	3	1.8	0.0	1.8	0.0	0.1
115	*Saxifraga*	SAXI	148	27.4	0.0	22.3	0.1	0.7
116	Liliaceae	LILI	235	41.5	0.0	30.6	0.2	1.2
117	*Bupleurum*	BUPL	23	11.4	0.0	3.2	0.0	0.1
118	Umbelliferae	UMBE	297	44.7	0.0	35.5	0.3	1.7
119	Cruciferae	CRUC	418	59.0	0.0	50.5	0.6	2.6
120	*Triglochin*	TRIG	6	4.0	0.0	2.2	0.0	0.1
121	*Thalictrum*	THAL	546	165.7	0.0	25.7	0.7	1.9
122	*Rumex*	RUME	40	3.2	0.0	15.0	0.0	0.4
123	*Polygonum*	POLG	590	98.2	0.0	77.8	1.1	3.9
124	Commelinaceae	COMM	3	2.5	0.0	0.4	0.0	0.0
125	*Typha*	TYPH	66	17.2	0.0	9.9	0.1	0.5
126	Sparganium	SPAR	15	10.9	0.0	0.8	0.0	0.0
127	*Sagittaria*	SAGI	3	2.2	0.0	0.6	0.0	0.0
128	*Acorus*	ACOR	3	2.0	0.0	1.2	0.0	0.0
129	*Alisma*	ALIS	11	5.7	0.0	1.3	0.0	0.0
130	Cyperaceae	CYPE	925	335.1	0.0	97.4	12.7	21.7
131	Myriophyllum	MYPL	164	58.1	0.0	15.8	0.2	0.8
132	*Nymphoides*	NYMP	21	5.2	0.0	5.6	0.0	0.2
133	Potamogeto	POTA	53	11.9	0.0	8.1	0.0	0.4
134	Onagraceae	ONAG	9	1.9	0.0	11.1	0.0	0.3
135	Palmae	PALM	1	1.0	0.0	0.8	0.0	0.0
136	Anacardiaceae	ANAC	53	8.2	0.0	10.8	0.0	0.3
137	*Platycarya*	PLAT	2	2.0	0.0	0.2	0.0	0.0
138	*Bombax*	BOMB	3	1.9	0.0	0.8	0.0	0.0
139	*Ailanthus*	AILA	3	2.7	0.0	0.4	0.0	0.0
140	*Lipuidambar*	LIPU	3	3.0	0.0	0.2	0.0	0.0
141	*Tetracentron*	TETR	1	1.0	0.0	0.9	0.0	0.0
142	*Cercidiphyllum*	CERO	1	1.0	0.0	0.4	0.0	0.0
143	Magnoliaceae	MAGN	1	1.0	0.0	0.3	0.0	0.0
144	*Mallothus*	MALL	3	1.6	0.0	2.6	0.0	0.1
145	*Macaranga*	MACA	4	2.4	0.0	2.4	0.0	0.1
146	Sterculiaceae	STER	5	3.3	0.0	0.8	0.0	0.0
147	Flacourtiaceae	FLAC	5	4.5	0.0	0.4	0.0	0.0
148	*Acacia*	ACAC	3	2.6	0.0	0.2	0.0	0.0

Table 1 (*continued*)

No.	Pollen Taxa	Taxa code	N[a]	Hill's N2[a]	Minimum	Maximum	Mean	Standard deviation
149	*Elaecarpus*	ELAE	1	1.0	0.0	0.8	0.0	0.0
150	*Alangium*	ALAN	1	1.0	0.0	0.2	0.0	0.0
151	*Ardisia*	ARDI	17	12.4	0.0	1.0	0.0	0.0
152	Campanulaceae	CAMP	7	6.3	0.0	0.4	0.0	0.0
153	*Phyllanthus*	PHYL	17	10.8	0.0	1.0	0.0	0.0
154	*Apodytes*	APOD	2	2.0	0.0	0.2	0.0	0.0
155	*Rhoiptelea*	RHOI	2	2.0	0.0	0.2	0.0	0.0
156	*Zanthoxylum*	ZANT	16	4.1	0.0	7.3	0.0	0.2
157	*Euptelea*	EUPT	1	1.0	0.0	0.1	0.0	0.0
158	*Olax*	OLAX	1	1.0	0.0	0.3	0.0	0.0
159	*Viburnum*	VIBU	39	9.3	0.0	6.3	0.0	0.2
160	*Coriaria*	CORI	7	5.3	0.0	0.6	0.0	0.0
161	*Saposhnikovia*	SAPO	9	7.4	0.0	0.6	0.0	0.0
162	Actinidiaceae	ACTI	9	6.2	0.0	0.7	0.0	0.0
163	*Akebia*	AKEB	1	1.0	0.0	0.2	0.0	0.0
164	Theaceae	THEA	4	3.3	0.0	0.4	0.0	0.0
165	*Eurya*	EURY	14	11.6	0.0	0.6	0.0	0.0
166	*Sanguisorba*	SAUG	12	11.0	0.0	0.4	0.0	0.0
167	*Schefflera*	SCHE	23	10.4	0.0	2.6	0.0	0.1
168	*Cuscuta*	CUSC	38	2.6	0.0	20.7	0.0	0.6
169	*Gynostemma*	GYNO	2	1.9	0.0	0.2	0.0	0.0
170	Bignoniaceae	BIGN	1	1.0	0.0	0.2	0.0	0.0
171	*Styrax*	STYR	1	1.0	0.0	0.4	0.0	0.0
172	*Melastoma*	MELA	4	2.9	0.0	1.2	0.0	0.0
173	*Mirabilis*	MIRA	1	1.0	0.0	0.2	0.0	0.0
174	*Quisqualis*	QUIS	1	1.0	0.0	0.1	0.0	0.0
175	*Lithospermum*	LITO	5	3.9	0.0	0.6	0.0	0.0
176	Amaranthaceae	AMAR	16	7.5	0.0	2.6	0.0	0.1
177	Mimosoideae	MIMO	6	5.3	0.0	0.4	0.0	0.0
178	*Prunella*	PRUN	17	10.9	0.0	1.3	0.0	0.1
179	Orchidaceae	ORCH	1	1.0	0.0	0.2	0.0	0.0
Spore Taxa								
180	Woodsiaceae	WOOD	3	2.1	0.0	4.1	0.0	0.1
181	*Selaginella*	SELA	196	23.0	0.0	88.7	0.8	6.0
182	*Selaginella-sinensis*	SSIN	42	5.1	0.0	90.8	0.3	4.1
183	*Pyrrosia*	PYRR	58	4.0	0.0	41.6	0.1	1.2
184	Polypodiaceae	PLYP	575	72.5	0.0	97.8	2.1	8.7
185	*Parathelypteris*	PARA	21	6.7	0.0	8.8	0.0	0.3
186	*Pteridium*	PTEX	5	3.8	0.0	2.4	0.0	0.1
187	*Pteris*	PTER	142	11.5	0.0	68.2	0.3	3.0
188	*Adiantum*	ADIA	249	44.7	0.0	31.2	0.2	1.1
189	Aspleniaceae	ASPL	3	2.0	0.0	1.1	0.0	0.0
190	*Athyrium*	ATHY	215	47.6	0.0	85.4	0.7	3.8
191	*Hicropteris*	HICR	19	8.2	0.0	1.4	0.0	0.1
192	*Osmunda*	OSMU	43	14.9	0.0	4.6	0.0	0.2
193	*Cyrtomium*	CYRT	4	2.5	0.0	3.3	0.0	0.1
194	*Dicranopteris*	DICR	3	2.8	0.0	3.9	0.0	0.1
195	*Dryopteris*	DRYO	4	2.0	0.0	2.9	0.0	0.1
196	*Hymenophyllum*	HYME	88	32.9	0.0	4.9	0.1	0.3
197	*Lycopodium*	LYCO	65	9.9	0.0	11.0	0.0	0.3
198	Plagiogyriaceae	PLAG	29	12.4	0.0	3.9	0.0	0.2
199	*Microlepia*	MICO	117	15.2	0.0	24.1	0.1	0.8
200	*Botrychium*	BOTR	15	7.2	0.0	2.4	0.0	0.1
201	*Dennstaedtia*	DENN	3	1.6	0.0	5.8	0.0	0.2
202	*Sinopteridaceae*	SINO	10	1.8	0.0	17.4	0.0	0.5
203	*Cryptogramma*	CRYP	33	16.7	0.0	1.8	0.0	0.1
204	Ophioglossaceae	OPHI	6	2.0	0.0	4.1	0.0	0.1
205	*Onychium*	ONYC	1	1.0	0.0	0.1	0.0	0.0
206	*Angiopteris*	ANGI	5	2.5	0.0	1.4	0.0	0.0
207	*Lepisorus*	LEPI	70	20.4	0.0	10.6	0.1	0.4
208	*Lygodium*	LYGO	3	1.4	0.0	3.6	0.0	0.1
209	*Cibotium*	CIBO	2	1.5	0.0	1.4	0.0	0.0
210	Davalliaceae	DAVA	13	1.7	0.0	15.7	0.0	0.4
211	*Nephrolepis*	NEPH	8	1.6	0.0	48.2	0.0	1.3
212	*Gymnocarpium*	GYMN	1	1.0	0.0	1.7	0.0	0.0
213	Other monolete spores	MONT	293	60.7	0.0	63.1	0.8	3.6
214	Other trilete spores	TRIL	90	15.7	0.0	36.8	0.2	1.8
215	Other unidentified	OTHE	111	43.1	0.0	18.0	0.2	1.3

[a] Pollen taxa number of occurrences (N) and effective number of occurrences (Hill's N2).

pCO_2, partial pressure of atmospheric carbon dioxide (PCO), mean annual precipitation (MAP), July precipitation (MP7), January precipitation (MP1), mean annual temperature (MAT), July temperature (MT7), January temperature (MT1), relative humidity (HHH), annual evaporation (EEE), >5 °C annual accumulated temperature (5CT), cloud cover (CCC), duration of sunlight (SSS), annual snow accumulation (SNO). Summary statistics for the 14 environmental variables are given in Table 2.

Table 2
Summary of the environmental characteristics in the 1202 studied sites used as possible explanatory variables for the distributions of surface-soil pollen.

Code Num	Code Name	Minimum	Maximum	Mean	Median	Standard deviation
1	ALT (m)	9.0	5484.0	3543.9	3700.0	1130.1
2	PCO (pa)	17.7	40.1	24.0	23.1	4.4
3	MAP(mm)	11.7	1842.6	499.8	435.5	302.0
4	MP7(mm)	3.8	371.9	113.1	107.9	65.1
5	MP1(mm)	0.4	24.3	3.9	3.0	3.3
6	MAT(°C)	−6.9	21.5	5.1	4.8	4.8
7	MT7(°C)	4.8	26.5	14.5	13.9	4.3
8	MT1(°C)	−21.4	14.3	−6.2	−7.5	6.0
9	HHH(1%)	23.3	82.4	54.6	53.6	10.0
10	EEE(mm)	961.1	3783.6	1824.5	1839.2	407.1
11	5CT(°C)	423.2	7278.7	2181.1	1839.6	1095.4
12	CCC(0.1)	34.8	82.1	55.7	54.9	8.5
13	SSS(h)	1187.3	3674.3	2623.2	2787.8	437.5
14	SNO(cm)	0.0	2006.7	153.9	71.9	242.4

3.3. Numerical analyses

Canonical ordination techniques, using the statistical program CANOCO version 4.5 (ter Braak, 1986,1988; ter Braak and Smilauer, 2002), were used to identify co-varying patterns between pollen assemblages and the 14 environmental variables. CANOCO was chosen as it employs several statistical methods for data analyses based on the characteristics of the dataset (e.g. linear or non-linear methods, direct or indirect analyses) (Jiang et al., 2001). We used detrended correspondence analysis (DCA-detrending by segments, non-linear rescaling of axes and down weighting of rare species) to determine which method was most appropriate with gradient length (range of variation) as the criterion (ter Braak, 1986,1988; ter Braak and Prentice, 1988). Non-linear methods (DCA and CCA) were appropriate for our pollen dataset, because the gradient lengths of standard deviation units were >2 (Birks, 1995).

Canonical Correspondence Analysis (CCA) was used to study the variation in biological assemblages that can be explained by a particular set of environmental variables. It can visualize complex pollen data and their relationships to the environmental variables (e.g. MAT, MAP). The resulting ordination diagrams of the CCA show the main pattern of variation in compositions of the biological assemblages as accounted for by the environmental variables and, in an approximate way, the distributions of the species along each environmental variable (ter Braak and Verdonschot, 1995).

The reconstruction technique used for all pass tests of environmental variables was locally weighted weighted averaging (LWWA) (Juggins, 2001) with the maximum number of sites available for each environmental variable. LWWA was used because it is a method that dynamically generates a “local” training set, which is optimized for each sample as it is based on the 30 closest analogs defined by the minimum squared chi-squared distance, and uses these in a weighted averaging reconstruction. Numerical comparisons have suggested that the LWWA approach can take advantage of the greater taxonomic diversity of the large training sets and avoid the problems of additional noise (Juggins, 2001; Rioual et al., 2007). The LWWA outperforms the traditional weighted averaging (WA) or WA-PLS techniques for the large merged datasets such as the one used here, and it is the recommended method for these (Juggins, 2001). The final LWWA model was selected that gave the lowest root mean squared error of prediction (s1 + s2) (bootstrap RMSEP), as assessed by the bootstrap method (Hall and Wilson, 1991) using C^2 version 1.5.1 (Juggins, 2003). The optima for the primary environmental variables of the main pollen species, presented in the modern dataset, were estimated by WA regression. Supplementary Data Table S1 shows the weighted-averaging environmental variables optima (WA opt.) and tolerances (WA tol.) of the 153 pollen taxa.

3.4. Data screening

In order to remove the effects of high collinearity among environmental variables in the process of analyses, we examined the Variance Inflation Factors (VIFs) for each environmental variable. If the VIF value of a variable was larger than 20, the variable was assumed to be almost perfectly correlated with the other variables and it captures little variance (ter Braak, 1988). After CCA analysis, the VIF values of both the altitude (ALT) and pCO2 variables were higher than 20. Thus we deleted the pCO2 variable. The remaining 13 environmental variables are interpreted to have a unique influence on pollen distribution (Fig. 5).

In all ordination analyses, samples that have extreme values in the explanatory variables have more influence on the results than

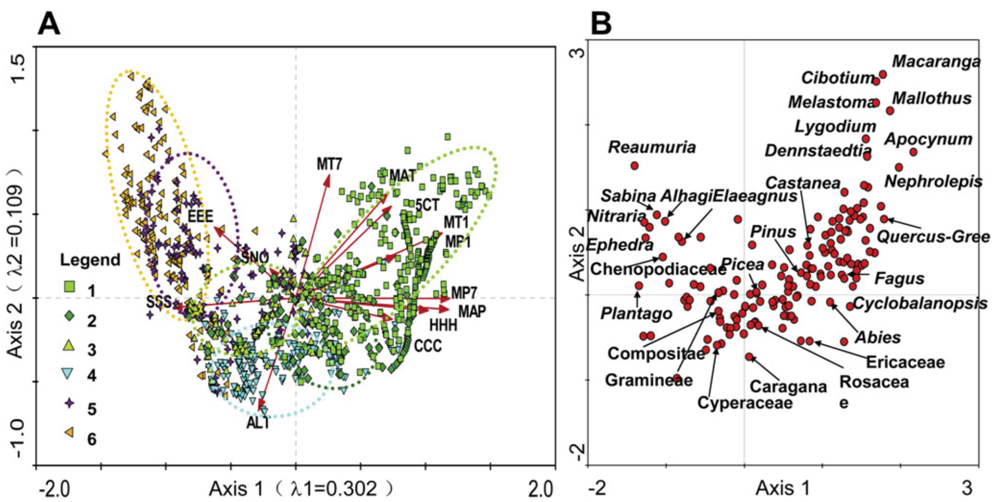

Fig. 5. Canonical correspondence analysis (CCA) showing the relationships between the 1188 sites (14 sites are passive) (A) and 13 environmental variables (B) and 153 pollen types (Eigenvalues: $\lambda_1 = 0.302$, $\lambda_2 = 0.109$). Abbreviation for environmental variables: ALT = Altitude; MAP = Mean annual precipitation; MP7 = July precipitation; MP1 = January precipitation; MAT = Mean annual temperature; MT7 = July temperature; MT1 = January temperature; HHH = Relative humidity; EEE = Annual evaporation; 5CT=>5 °C accumulated temperature annually; CCC = Cloud cover; SSS = Duration of sunlight; SNO = Annual snow accumulation. Legend, 1 = Forest, 2 = Scrub, 3 = Steppe, 4 = Alpine meadow, 5 = Desert steppe, and 6 = Desert and alpine desert.

those of central samples (ter Braak, 1994). The extremity of the position of the samples in the space of environmental variables was examined using leverage diagnostics in CCA (ter Braak and Smilauer, 2002). We deleted all samples which have environmental variables with greater than eight times the average leverage from further analysis (Weckström et al., 1997; ter Braak and Smilauer, 2002). Eighteen samples (No. 11, 18, 34, 53, 65, 112, 137, 182, 267, 1166, 1170, 1185, 1187, 1188, 1192, 1193, 1199, and 1202) were identified as outliers based on their unusual statistical characteristics. These outlying samples were included as passive samples in the ordination analyses (Fig. 5).

3.5. Reconstruction of a fossil sequence

Lake Chen Co (28°53′–59′N, 90°33′–39′E; elevation 4420 m asl) is located in a hydrologically closed basin (Fig. 4). The maximum length, width, and depth are 11,000, 7800, and 31 m, respectively. The lake area is about 38 km^2, while the drainage basin is about 148 km^2 (Zhu et al., 2009).

Chen Co is located in a subalpine temperate, semi-arid region of the north Himalayan main range, thus in a rain-shadow area of the Indian monsoon, where the rainy season is mainly from June to September. Mean annual precipitation (MAP) is 372 mm and mean annual temperature (MAT) is 2.4 °C, July temperature (MT7) is 11.3 °C. High insolation and strong winds result in a mean annual evaporation (EEE) as high as ca. 2050 mm and relative humidity (HHH) about ca. 51% (China Meteorological Administration (CMA); Liu, 1995). The surrounding vegetation is alpine meadow-steppe (ITCAS, 1988; Zhu et al., 2009).

A sediment core (TC1) measuring 36.7 m in length and AMS ^{14}C dated to the last 30,000 years has been successfully used for palaeoclimatic reconstruction (Zhu et al., 2009). From the original data (Zhu et al., 2009), we selected 116 pollen samples from the uppermost 12.50 to 3 m of the TC1 core (as the above 3 m sediments are redeposited), which spans ~10,700–3200 cal yr BP, for the quantitative reconstruction of Holocene climatic changes in southern Tibet.

4. Results

4.1. Modern pollen assemblages

The pollen assemblages, consisting of a total of 153 taxa, of the 1202 surface samples are summarized in Fig. 6. Overall, the modern pollen assemblages from different vegetation types across the Qinghai-Tibetan Plateau are remarkably distinct from each other.

The modern pollen assemblages from forest zone are dominated by *Abies* (max.72%), *Picea* (max.68%), *Pinus* (40 ± 30%), *Betula* (max.51%), and *Quercus* (max.67%). Polypodiaceae is consistently present and very frequent (up to 98%) in many samples. These pollen-spore types have a symmetric unimodal response model with the highest values occurring in warm temperate deciduous forest to subalpine dark coniferous forest in the southeastern and eastern parts of the Tibetan Plateau.

Ericaceae (max. 80%, avg. 8.7 ± 17%), Rosaceae (max.29%, avg. 4 ± 5.7%), *Pinus* (max.83%, avg. 20 ± 18%), *Artemisia* (max.41%, avg. 10 ± 10%), and Composite (Asteraceae) (max.21%, avg. 3 ± 4.2%) are in relatively high abundance in scrub areas. For the steppe areas, Gramineae (Poaceae) (max.62.7%, avg. 12.1 ± 15.9%), Chenopodiaceae (max.25.2%, avg. 5.5 ± 6.7%), *Artemisia* (max.75%, avg.29.5 ± 20.1%), Composite (max.39.8%, avg. 5.3 ± 6.2%), and Cyperaceae (max.46%, avg.12.8 ± 11.3%) are most common in steppe sites.

Cyperaceae reach a maximum value of 97.4% (avg. 45.2 ± 25.5%), with generally low (max.33.8%, avg. 4.3 ± 5.4%) and fluctuating Gramineae in alpine meadow between elevation ca. 3000 and ca.5000 m covering the east-central parts of the Tibetan Plateau (Fig. 7A,B). *Artemisia* (max.97.8%, avg. 47.5 ± 25.1%), *Arenaria* (max.88.8%, avg. 4.7 ± 13.1%), and Chenopodiaceae (max.89.8%, avg. 13.3 ± 13.0%) pollen are most common in desert steppe. Chenopodiaceae (avg.47 ± 25.0%), *Ephedra* (max.85.1%, avg.8.3 ± 13.6%), and *Nitraria* (max.98.9%, avg.3.5 ± 10.1%) pollen increase steadily toward drier regions, which are mostly covered by desert and alpine desert.

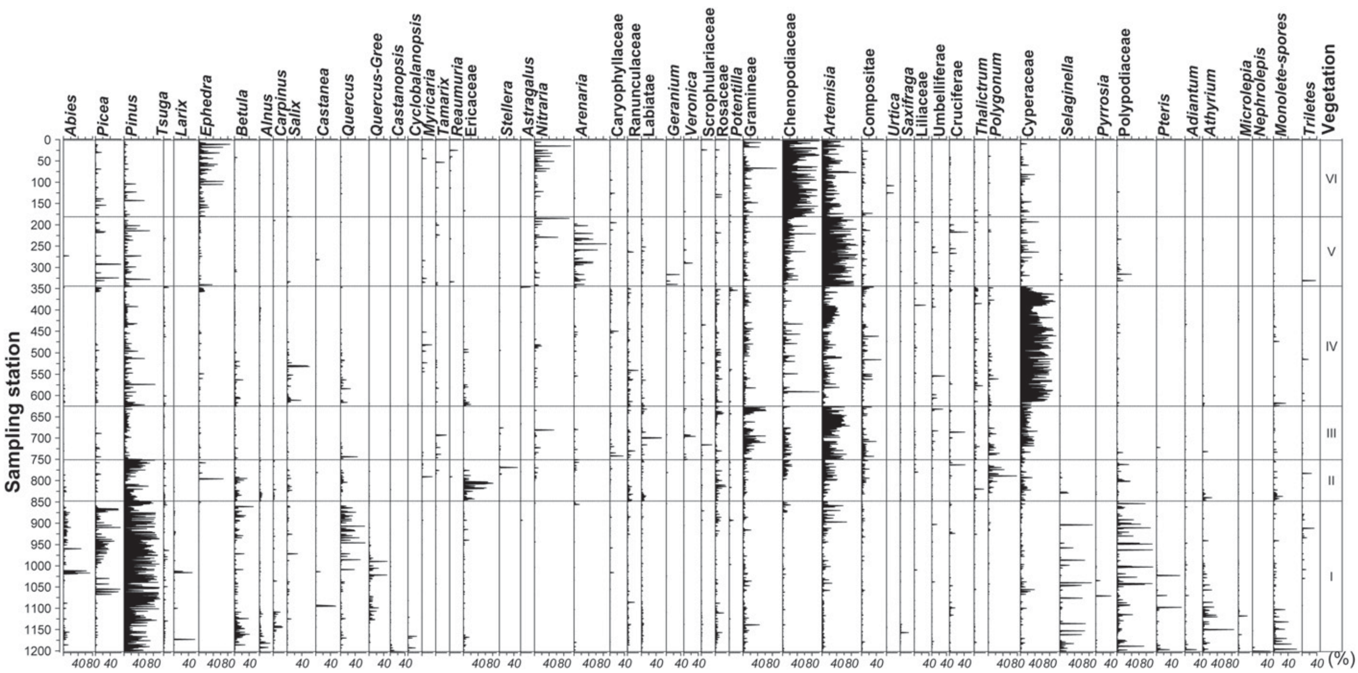

Fig. 6. Pollen diagram for the Qinghai-Tibetan Plateau surface soil samples, showing the percentage values for selected pollen and spore taxa. The samples are arranged according to 6 vegetation types from I-Forest (bottom), II-Scrub, III-Steppe, IV-Alpine meadow, V-Desert steppe, to VI-Desert and alpine desert (top).

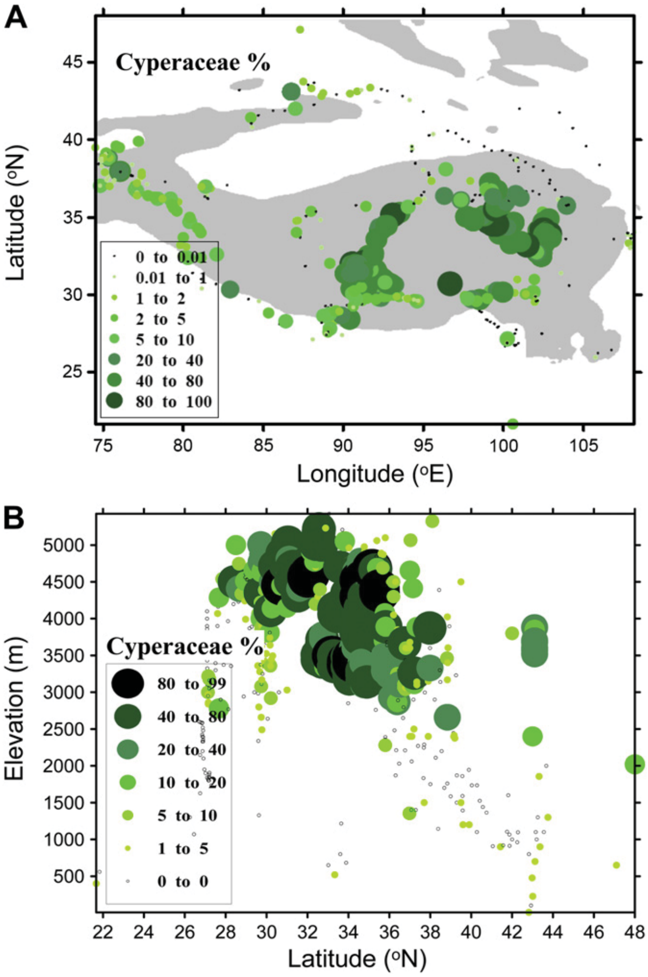

Fig. 7. Spatial distribution patterns of Cyperaceae pollen. A, Scatter plots relating percentages of Cyperaceae pollen against Latitude (°N), Longitude (°E); B, Scatter plots relating percentages of Cyperaceae pollen against Elevation (m), Longitude (°E). Size of colored dots is proportional to percentage of the Cyperaceae pollen in the sample.

4.2. Ordination analyses

The eigenvalues of the first two CCA axes are $\lambda_1 = 0.302$ and $\lambda_2 = 0.109$, and the species-environment correlations for the same axes are high (0.91, 0.71), indicating a strong relationship between the distribution of the 153 pollen types and the 13 environmental variables (Table 3, Fig. 5).

The CCA species – and sample– environment biplots are shown in Fig. 5. In the biplot, the length of the arrows for the environmental variables roughly corresponds to their relative importance in pollen variance, and their orientation shows their approximate correlations to ordination axes and the other environmental variables. MAP is closely related to HHH since there is only a small angle between the arrows of MAP and HHH (Fig. 5A). ALT is negatively correlated with MT7. Pollen-spore taxa preferring high MAP and MAT are generally positioned to the upper right of the CCA biplots (Fig. 5B) (e.g. *Macaranga*, *Mallothus*, *Melastoma*, *Cibotium*, *Lygodium*, and *Quercus-Evergreen*). They are in highest abundance at sites in the southern foothill of the Himalayas and the southeastern low altitude areas of Tibetan Plateau, where tropical evergreen monsoon rainforest and mixed subtropical evergreen and deciduous forest dominate (Fig. 5B). Pollen-spore types situated in the right of the biplots are *Castanea*, *Pinus*, *Fagus*, *Picea*, and *Abies*, which have the highest abundance in the temperate deciduous forest and subalpine dark coniferous forests of the Qinghai-Tibetan Plateau. Pollen-spore types positioned near the center of the biplots (Fig. 5B) are Ericaceae, Rosaceae, *Caragana*, *Artemisia*, Gramineae, Composite, Cyperaceae, which have the highest abundance in the alpine meadow, steppe and mixed alpine scrub in the Plateau.

In contrast to the relatively warm taxa above, pollen placed to the left of the CCA biplots are relatively dry and cold taxa, such as *Reaumuria*, *Sabina*, *Alhagi*, *Nitraria*, *Ephedra*, and Chenopodiaceae (Fig. 5A,B). These pollen types are mainly found in desert steppe and alpine desert occurring in the north and northwest regions of the Qinghai-Tibetan Plateau. From the upper left to the lower right gradients of the CCA biplots, which nearly parallel the EEE and HHH reversed arrows, the environmental gradient changes from relatively dry to relatively wet conditions. This climatic gradient broadly corresponds to the vegetation changes from alpine desert to steppe to alpine meadow and to conifer forest.

Table 3
Summary statistics for the first four axes of CCA, with 1188 active sites (14 sites are passive), 153 pollen types, and 13 environmental variables.

	Axis 1	Axis 2	Axis 3	Axis 4	Total inertia	Conditional effects		
						Lambda A	P	F
Eigenvalues	0.302	0.109	0.061	0.044				
Species-environment correlations	0.912	0.707	0.618	0.551				
Cumulative percentage variance								
of species data	9.2	12.5	14.3	15.7				
of species-environment relation	49.4	67.2	77.2	84.4				
Sum of all eigenvalues					3.296			
Sum of all canonical eigenvalues					0.612			
Inter-set correlation of significant environmental variables with axes								
ALT (m) (altitude)	−0.21	−0.73	−0.36	0.10		0.03	0.002	11.68
MAP (mm) (annual mean precipitation)	0.86	−0.07	0.40	−0.09		0.24	0.002	90.84
MP7 (mm) (July precipitation)	0.87	0.00	0.15	0.32		0.03	0.002	9.78
MP1 (mm) (January precipitation)	0.56	0.27	0.00	0.36		0.01	0.002	6.55
MAT (°C) (annual mean temperature)	0.52	0.67	0.14	−0.15		0.08	0.002	31.34
MT7 (°C) (July temperature)	0.19	0.79	0.24	−0.29		0.01	0.002	2.79
MT1 (°C) (January temperature)	0.82	0.42	0.08	0.02		0.08	0.002	35.33
HHH (%) (relative humidity)	0.75	−0.08	0.18	−0.28		0.04	0.002	16.84
EEE (mm) (annual evaporation)	−0.46	0.45	−0.37	0.15		0.03	0.002	13.58
5CT (°C) (>5 °C accumulated temperature annually)	0.54	0.59	0.02	−0.32		0.03	0.002	8.97
CCC (0.1) (Cloud cover)	0.54	−0.14	0.38	−0.29		0.01	0.002	8.26
SSS (h) (sunlight times)	−0.69	−0.06	−0.28	0.36		0.02	0.002	4.87
SNO (cm) (annual accumulate depth of snow)	−0.15	0.19	0.21	0.20		0.01	0.002	6.03

Monte Carlo permutation tests (499 unrestricted permutations) of the first two axes indicate that both are statistically significant ($p < 0.01$). Forward selection and unrestricted Monte Carlo permutation tests show that main environmental variables (MAP, MT1, MAT, ALT, HHH, EEE, CCC, and MP7, etc.) are statistically significant in relation to the variance in the pollen data ($p < 0.01$, 499 permutations, Table 3), capturing more than 88% of the total variance. MAP alone captures nearly half of the 88% (MAP, 0.24), suggesting that MAP is the most important environmental factor and has the largest influence on pollen distribution in the Qinghai-Tibetan Plateau.

Collectively, the environmental variables explain 18.6% of the variation in the pollen data (Table 3). The low percentage variance explained is typical of such noisy datasets with large numbers of taxa and many zero values in the species matrix (ter Braak, 1986; Bennion, 1994; Jongman et al., 1995). A series of partial CCAs with one variable as explanatory and with others as covariables at a time, was used to abstract the unique contribution of individual environmental variable to pollen information (Borcard et al., 1992). Partial CCAs show that 4.4% of this variance can be explained by ALT, 4.9% by MAP, 6.2% by HHH, 3.3% by MT1, 3.0% by EEE, 3.0% by CCC, 2.5% by MP7, and 2.0% by MAT. Total intercorrelation between environmental variables is responsible for 61.8% of the explained variance (Fig. 8).

The associated Monte Carlo permutation tests demonstrate that the relationship between pollen species and each environmental variable is significant ($p = 0.002$) (Table 3) and, each of these environmental gradients accounted for a significant portion of the total variance in the pollen data. Therefore, the relationship between pollen distributions and environmental variables of the MAP, MAT, MT1, ALT, HHH, EEE, MP7, and CCC, etc. in this dataset is sufficiently robust to develop the regional environmental transfer functions that will assist to reconstruct quantitatively palaeoenvironmental parameters using the pollen records of sediments in the Qinghai-Tibetan Plateau.

4.3. *Transfer function development*

According to the performance of several environmental transfer functions developed (Table 4), the locally weighted weighted averaging (LWWA) model (Juggins, 2001) appears better than WA, WA-PLS, and MAT (Modern Analog Technique), since it shows the highest R^2 Boot value and the lowest RMSEP-Boot.

Comparisons of the observed and predicted variables from the analysis indicate that the performance of each model was usually particularly poor for a few samples with very high residuals. These

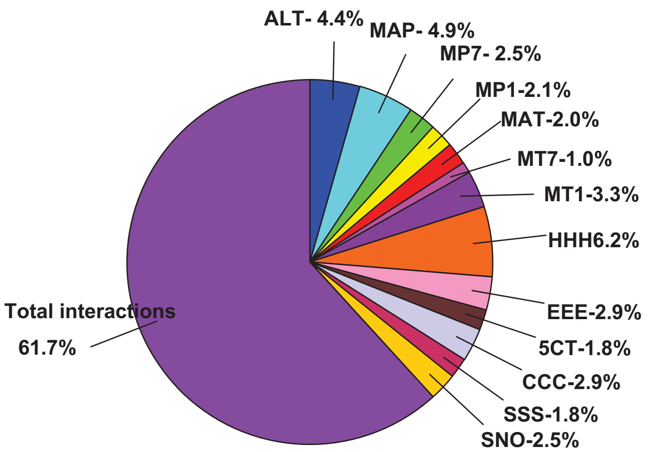

Fig. 8. Pie charts showing the components representing the unique contributions of the main environmental variables and the interaction between variables.

Table 4
Error estimates for different calibration models. Model errors are given as root mean square errors (RMSE) and prediction errors as root mean square errors of prediction (RMSEP (boot)) calculated by bootstrapping. In addition, the adjusted coefficients of determination R^2 (boot) between bootstrap predicted and observed values are given.

Model	Method	RMSE	R^2	Boot_R^2	RMSEP (boot)	RMSEP as % of gradient
MAP (mm)	WA_Inv	152	0.73	0.72	156	
	WA_Cla	177	0.73	0.72	178	
	WATOL_Inv	151	0.74	0.74	162	
	WATOL_Cla	176	0.74	0.74	184	
	WA_PLS Component 1	154	0.73	0.72	157	
	WA_PLS Component 2	132	0.80	0.77	143	
	WA_PLS Component 3	124	0.82	0.79	141	
	WA_PLS Component 4	120	0.84	0.78	145	
	WA_PLS Component 5	118	0.84	0.78	151	
	MAT	113	0.86	0.86	121	
	WMAT	110	0.86	0.86	118	
	LWWA_Inv	**51**	**0.97**	**0.89**	**109**	**5.9 % (109/1831)**
	LWWA_Cla	55	0.97	0.89	111	
MAT (°C)	WA_Inv	3.0	0.57	0.55	3.1	
	WA_Cla	4.0	0.57	0.55	4.0	
	WATOL_Inv	3.1	0.54	0.55	3.2	
	WATOL_Cla	4.3	0.54	0.55	4.1	
	WA_PLS Component 1	3.0	0.57	0.55	3.1	
	WA_PLS Component 2	2.7	0.66	0.63	2.9	
	WA_PLS Component 3	2.5	0.70	0.64	2.9	
	WA_PLS Component 4	2.5	0.72	0.63	3.0	
	WA_PLS Component 5	2.4	0.73	0.62	3.1	
	MAT	2.3	0.74	0.74	2.5	
	WMAT	2.3	0.75	0.75	2.4	
	LWWA_Inv	**1.1**	**0.94**	**0.78**	**2.3**	**8.1% (2.3/28.4)**
	LWWA_Cla	1.2	0.94	0.78	2.4	
MT1 (°C)	WA_Inv	3.0	0.73	0.72	3.1	
	WA_Cla	3.5	0.73	0.72	3.6	
	WATOL_Inv	3.1	0.72	0.72	3.2	
	WATOL_Cla	3.6	0.72	0.72	3.6	
	WA_PLS Component 1	3.0	0.78	0.71	3.1	
	WA_PLS Component 2	2.7	0.78	0.75	2.9	
	WA_PLS Component 3	2.6	0.80	0.75	3.0	
	WA_PLS Component 4	2.5	0.82	0.75	3.1	
	WA_PLS Component 5	2.5	0.82	0.74	3.2	
	MAT	2.5	0.81	0.81	2.7	
	WMAT	2.5	0.81	0.81	2.6	
	LWWA_Inv	**1.2**	**0.96**	**0.84**	**2.5**	**7% (2.5/35.7)**
	LWWA_Cla	1.2	0.95	0.84	2.6	
MT7 (°C)	WA_Inv	2.9	0.51	0.49	3.0	
	WA_Cla	4.1	0.51	0.49	4.0	
	WATOL_Inv	3.2	0.42	0.40	3.3	
	WATOL_Cla	4.9	0.42	0.40	5.0	
	WA_PLS Component 1	2.9	0.51	0.49	3.0	
	WA_PLS Component 2	2.6	0.60	0.57	2.8	
	WA_PLS Component 3	2.4	0.65	0.59	2.8	
	WA_PLS Component 4	2.4	0.68	0.59	2.8	
	WA_PLS Component 5	2.3	0.69	0.58	2.9	
	MAT	2.2	0.72	0.72	2.3	
	WMAT	2.2	0.73	0.73	2.3	
	LWWA_Inv	**1.0**	**0.95**	**0.78**	**2.1**	**9.7% (2.1/21.7)**
	LWWA_Cla	1.0	0.94	0.78	2.2	
ALT (m)	WA_Inv	762	0.48	0.46	782	
	WA_Cla	1100	0.48	0.46	1076	
	WATOL_Inv	798	0.43	0.43	831	
	WATOL_Cla	1213	0.43	0.43	1208	
	WA_PLS Component 1	764	0.48	0.46	787	
	WA_PLS Component 2	677	0.59	0.56	717	
	WA_PLS Component 3	642	0.63	0.57	715	
	WA_PLS Component 4	622	0.66	0.57	734	
	WA_PLS Component 5	608	0.67	0.56	759	
	MAT	603	0.68	0.68	636	
	WMAT	590	0.69	0.69	624	
	LWWA_Inv	**267**	**0.94**	**0.73**	**597**	**11% (597/5475)**
	LWWA_Cla	282	0.92	0.71	609	

(*continued on next page*)

Table 4 (*continued*)

Model	Method	RMSE	R^2	Boot_R^2	RMSEP (boot)	RMSEP as % of gradient
HHH (%)	WA_Inv	6.1	0.60	0.59	6.2	
	WA_Cla	7.8	0.60	0.59	7.8	
	WATOL_Inv	6.1	0.60	0.59	6.5	
	WATOL_Cla	7.8	0.60	0.59	8.3	
	WA_PLS Component 1	6.1	0.60	0.59	6.2	
	WA_PLS Component 2	5.2	0.71	0.67	5.7	
	WA_PLS Component 3	5.0	0.73	0.68	5.6	
	WA_PLS Component 4	4.9	0.75	0.69	5.7	
	WA_PLS Component 5	4.8	0.76	0.68	5.9	
	MAT	4.5	0.78	0.78	4.8	
	WMAT	4.4	0.79	0.79	4.7	
	LWWA_Inv	**2.0**	**0.96**	**0.82**	**4.5**	**7.6%(4.5/59)**
	LWWA_Cla	2.0	0.96	0.82	4.6	
MP7 (mm)	WA_Inv	29	0.78	0.76	30	
	WA_Cla	33	0.78	0.76	33	
	WATOL_Inv	30	0.75	0.75	34	
	WATOL_Cla	35	0.75	0.75	39	
	WA_PLS Component 1	29	0.78	0.76	30	
	WA_PLS Component 2	26	0.82	0.79	28	
	WA_PLS Component 3	24	0.84	0.80	29	
	WA_PLS Component 4	24	0.85	0.80	29	
	WA_PLS Component 5	23	0.86	0.79	31	
	MAT	25	0.83	0.84	26	
	WMAT	25	0.84	0.84	26	
	LWWA_Inv	**10**	**0.97**	**0.87**	**23**	**6.3% (23/368)**
	LWWA_Cla	10	0.97	0.87	24	
EEE (mm)	WA_Inv	295	0.40	0.38	301	
	WA_Cla	467	0.40	0.38	465	
	WATOL_Inv	293	0.40	0.38	314	
	WATOL_Cla	468	0.40	0.38	488	
	WA_PLS Component 1	295	0.40	0.38	301	
	WA_PLS Component 2	257	0.54	0.50	276	
	WA_PLS Component 3	241	0.60	0.52	275	
	WA_PLS Component 4	231	0.63	0.52	280	
	WA_PLS Component 5	228	0.64	0.51	289	
	MAT	218	0.67	0.67	231	
	WMAT	211	0.69	0.69	225	
	LWWA_Inv	**96**	**0.94**	**0.73**	**215**	**7.6% (215/2822)**
	LWWA_Cla	97	0.93	0.72	221	
CCC (0.1)	WA_Inv	6.3	0.41	0.38	6.5	
	WA_Cla	9.8	0.41	0.38	9.7	
	WATOL_Inv	6.3	0.42	0.41	6.6	
	WATOL_Cla	9.7	0.42	0.41	9.8	
	WA_PLS Component 1	6.3	0.41	0.39	6.5	
	WA_PLS Component 2	5.5	0.56	0.49	6.0	
	WA_PLS Component 3	5.1	0.61	0.52	6.0	
	WA_PLS Component 4	4.9	0.64	0.52	6.1	
	WA_PLS Component 5	4.8	0.66	0.51	6.3	
	MAT	4.4	0.72	0.72	4.7	
	WMAT	4.3	0.74	0.73	4.5	
	LWWA_Inv	**1.9**	**0.95**	**0.77**	**4.3**	**9.1%(4.3/47)**
	LWWA_Cla	2.0	0.94	0.77	4.4	

Abbreviations: WA, weighted average; WA-Tol, weighted average (tolerance down weighted); WA-PLS, weighted averaging partial least squares; WMAT, modern analog technique (weighted average of 30 closest analogues).

were removed by using the following screening techniques of the outlier samples. Locally weighted weighted averaging (LWWA) and modern analog technique (MAT) using the weighted average of the 30 nearest analogs were employed to remove data with high residuals. The results of model tests are summarized in Table 4.

Best significant relationships were established between pollen assemblages and MAP (R^2-boot = 0.89, RMSEP = 109 mm), MAT (R^2-boot = 0.78, RMSEP = 2.3 °C), MT1 (R^2-boot = 0.84, RMSEP = 2.5 °C), ALT (R^2-boot = 0.73, RMSEP = 597m), HHH (R^2-boot = 0.82, RMSEP = 4.5%), MP7 (R^2-boot = 0.87, RMSEP = 23 mm), EEE (R^2-boot = 0.73, RMSEP = 215 mm), CCC (R^2-boot = 0.77, RMSEP = 4.3) (Table 4).

The results of the LWWA model for pollen-inferred MAP, MAT, HT1, ALT, HHH, MP7, EEE, and CCC with plots of predicted (bootstrapping) against observed values are shown in Fig. 9A,B. The statistical correlation of modern meteorological data with those predicted by the pollen–climate calibration sets in the statistical bootstrap cross-validation reflects the inference power of the dataset.

4.4. Fossil record and transfer functions application

The pollen spectra from Chen Co Lake are dominated by herbaceous pollen such as Gramineae (Poaceae), *Artemisia*, Composite, Cyperaceae, *Thalictrum*, Chenopodiaceae, and Umbelliferae. The arboreal pollen contains mainly grains of *Pinus* and *Betula*, along with isolated grains of *Abies, Picea,* and *Tsuga*. The Holocene pollen record of the Chen Co Lake is divided into three pollen zones (Fig. 10).

Zone III (1250–1040 cm; 10,700–9040 cal a BP). *Artemisia* pollen is consistently and abundantly present throughout this zone. Its percentage varies between 30% and 80%. Gramineae pollen fluctuates between 5% and 20% with one peak (52.9%) at ca. 9360 cal a BP. Cyperaceae pollen declines sharply from 60% at the bottom to zero. This zone has high *Pinus* (max.31.6%) and Chenopodiaceae (max.20%).

Zone II (1040–661 cm; 9040–6050 cal a BP). Cyperaceae pollen abruptly increases from 20% to 80%, whereas *Pinus*, Chenopodiaceae, Gramineae, and *Artemisia* pollen decreases markedly. *Betula* and Umbelliferae are more prevalent in this zone than in the rest of the sequence.

Zone I (661–300 cm; 6050–3200 cal a BP). Cyperaceae pollen unsteadily decreases to low percentages (10–30%). *Artemisia* pollen increases first, followed by the pollen of the hydrophyte *Myriophyllum* which dramatically reaches its highest levels (max. 53.3%) at ca. 5000 cal a BP. Rosaceae and Composite pollen show a generally increasing trend.

The results of the MAP, MAT, HHH, and EEE reconstruction by transfer functions are consistent in showing warm and arid conditions during the very early Holocene (pollen Zones III) and relatively wetter conditions during the early to middle Holocene (pollen Zones II) (Fig. 10).

Fig. 11 shows that the climate between 10,700 and 9040 cal a BP was warm and dry with MAT around avg.3.2 °C, MAP around 354 ± 78 mm, HHH around 49 ± 4%, EEE around 2010 ± 270 mm, as reconstructed with transfer function. The maximum MAT reached about 6.0 °C, significantly higher than the present value (2.4 °C).

The climate shifted to humid or wet conditions toward the middle Holocene (from 9040 to 6050 cal a BP). In this interval, MAP fluctuated around 400 mm, obviously higher than the preceding interval and higher than the present except for a short fluctuation. A relatively humid phase appeared around 8600 cal a BP with HHH averaged around 53 ± 2.6% and the maximum HHH around 60%. Reconstructed MAT after 7200 cal a BP is lower than that of today. Relatively low EEE, about 1790 ± 137 mm, also occurred in this interval. After 6050 cal a BP, MAP decreased gradually to ca. 340 mm, which is slightly below the present value (372 mm).

5. Discussion

5.1. Climatic and environmental optima for pollen taxa

The Quaternary pollen records from the Tibetan Plateau have greatly increased in recent years. However, the detailed interpretation of pollen data has often been neglected because of the lack of plant ecological knowledge, especially of detailed optima and tolerances of climate environment variables (e.g. MAT, MAP) for the typical pollen taxa.

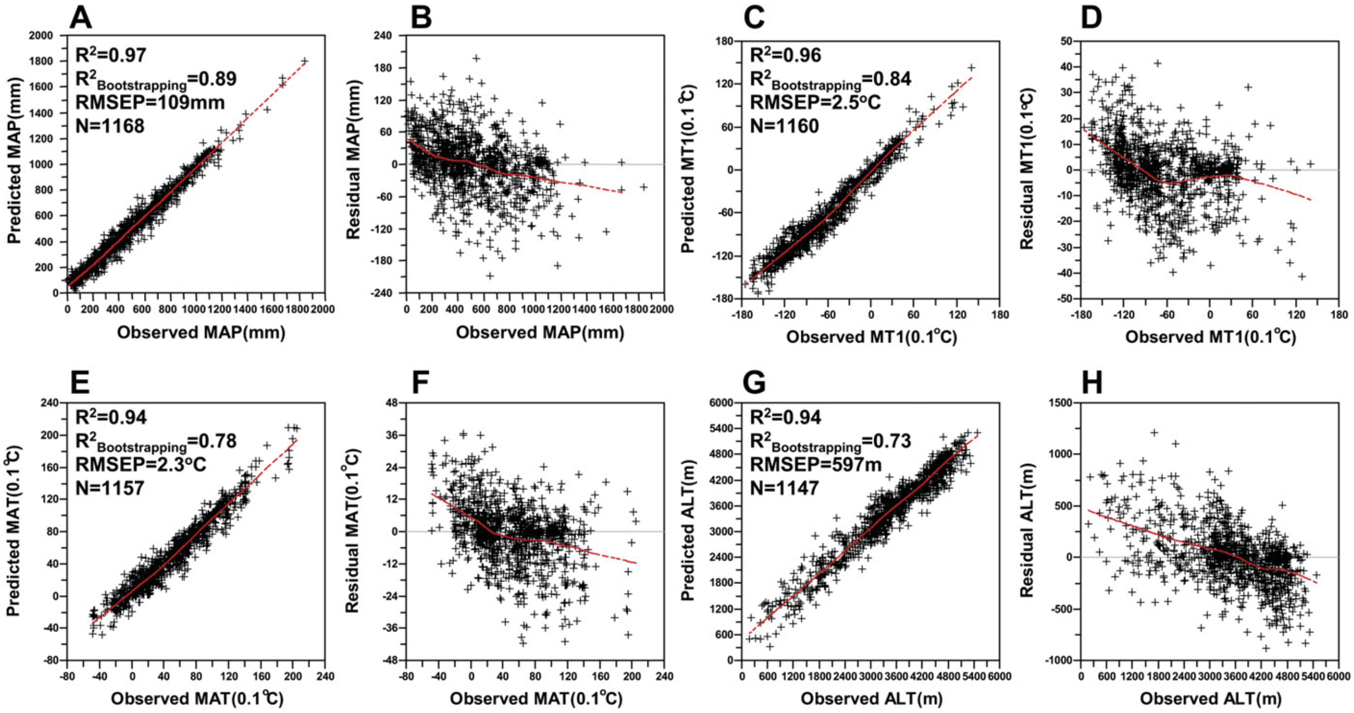

Fig. 9. A) Plots of LWWA inference model, showing (A) pollen predicted MAP values vs. observed MAP values, and (B) residuals vs. observed MAP values; (C) pollen predicted MT1 values vs. observed MT1 values, and (D) residuals vs. observed MT1 values; (E) pollen predicted MAT values vs. observed MAT values, and (F) residuals vs. observed MAT values; (G) pollen predicted ALT values vs. observed ALT values, and (H) residuals vs. observed ALT values.

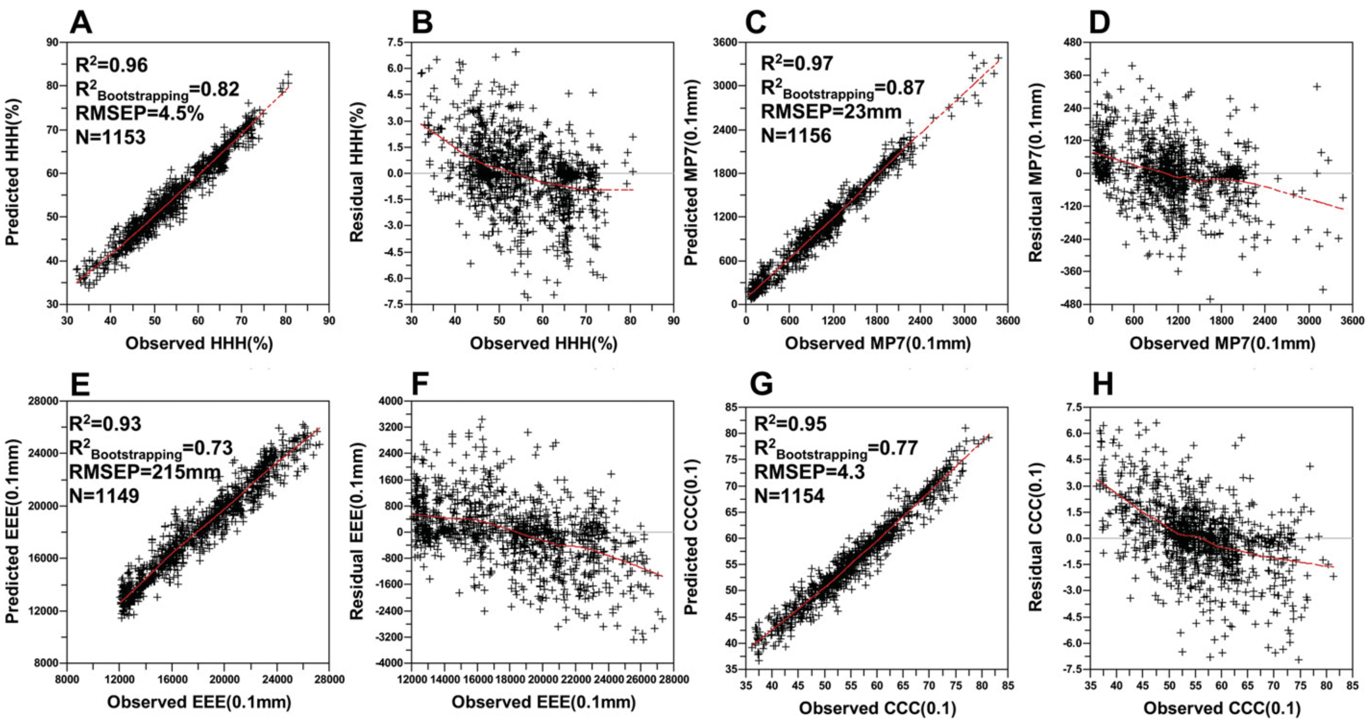

Fig. 9. B) Plots of LWWA inference model, showing (A) pollen predicted HHH values vs. observed HHH values, and (B) residuals vs. observed HHH values; (C) pollen predicted MP7 values vs. observed MP7 values, and (D) residuals vs. observed MP7 values; (E) pollen predicted EEE values vs. observed EEE values, and (F) residuals vs. observed EEE values; (G) pollen predicted CCC values vs. observed CCC values, and (H) residuals vs. observed CCC values.

Fig. 12 shows the weighted-average optima and tolerances for MAT, MAP, and ALT of the selected pollen taxa in the Qinghai-Tibetan Plateau. The detailed optima and tolerances to more environmental variable also are shown in the supplementary data Table S1.

Pollen taxa with the lowest MAT optima (ca.2–3.5 °C), such as Cyperaceae, *Arenaria*, Caryophyllaceae, *Thalictrum*, and *Androsace* (Fig. 12A), display the moderate MAP optima ranges (ca.420–550 mm), and highest altitude optima (ca.3900–4300 m)

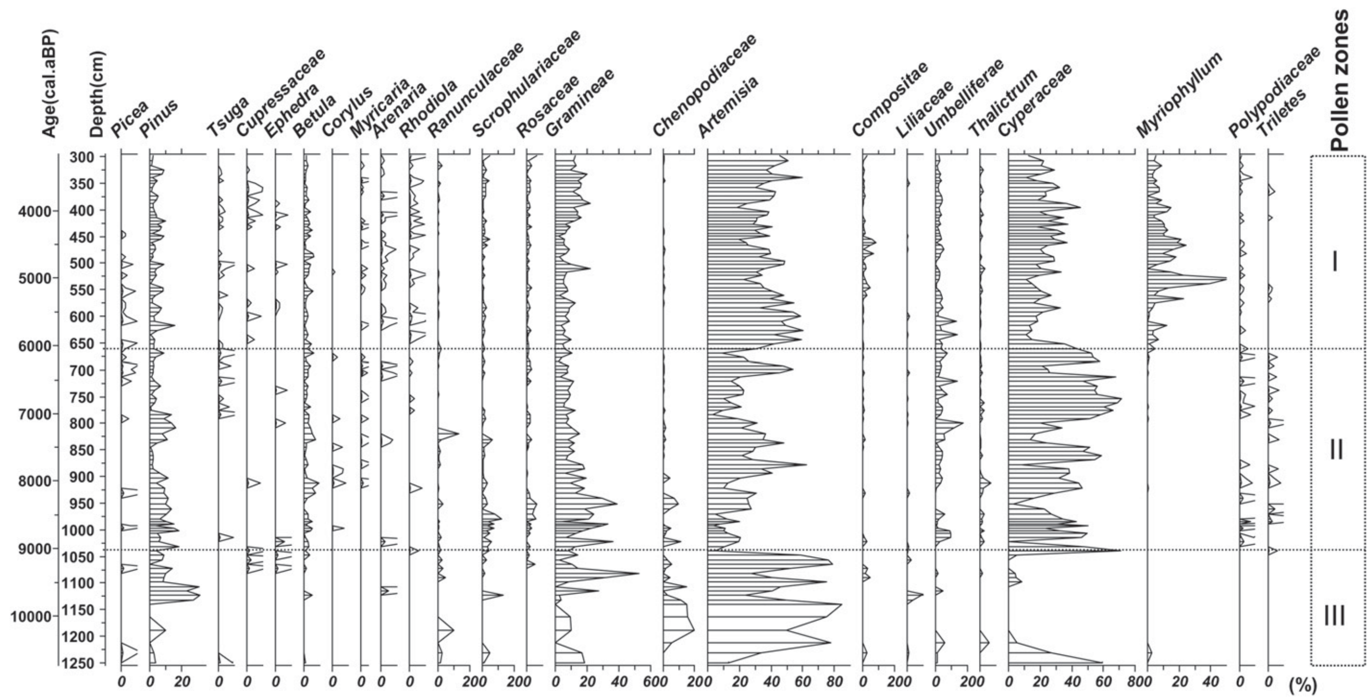

Fig. 10. Pollen diagram from the Chen Co Lake, southern Qinghai-Tibetan Plateau, China, presented on depth and calibrated-age scales.

(Fig. 12B), which closely reflect the geographical and climatic distribution of the alpine meadow in the Qinghai-Tibetan Plateau (ITCAS, 1988; Institute of Geography, 1990, 1999).

Estimated lower MAP optima for *Reaumuria* (200 mm), *Ephedra* (240 mm), *Nitraria* (270 mm) has similar narrow tolerances ranges of ca.130 mm, while Chenopodiaceae has optimum of 295 mm, and tolerance of 160 mm. There is also a good agreement with those species found at the lower MAP areas of at desert and alpine desert in the Qinghai-Tibetan Plateau (ITCAS, 1988).

Lu et al. (2008) has highlighted the optima of ALT, MAT and MAP for both *Abies* and *Picea* by using 857 surface samples datasets in the Qinghai-Tibetan Plateau, which are consistent with our new results on the basis of 1202 surface samples. The optima ALT of both *Abies* and *Picea* (Fig. 12A,B) are from ca.3300–3600 m, MAT from ca. 5.9–7.9 °C, and MAP from ca. 540–710 mm.

A number of pollen taxa in datasets display the warm (MAT optima > 10 °C), and moist (MAP optima >1000 mm) ranges, such as *Lygodium*, Acanthaceae, *Castanopsis*, and *Fagus* (Fig. 12A,B). They are highly correlated with modern distribution of these taxa, which is largely controlled by lower elevation and strong monsoon climate in the southern foothill of the Himalayas and in the southeastern Tibetan Plateau (ITCAS, 1988).

In the Qinghai-Tibetan Plateau, the plant taxonomy is extremely diverse. The taxonomic list of plant types that have been recorded contains more than 1200 genera, including ca. 5700 species (ITCAS, 1988). However, a lot of pollen was only identified to the family or

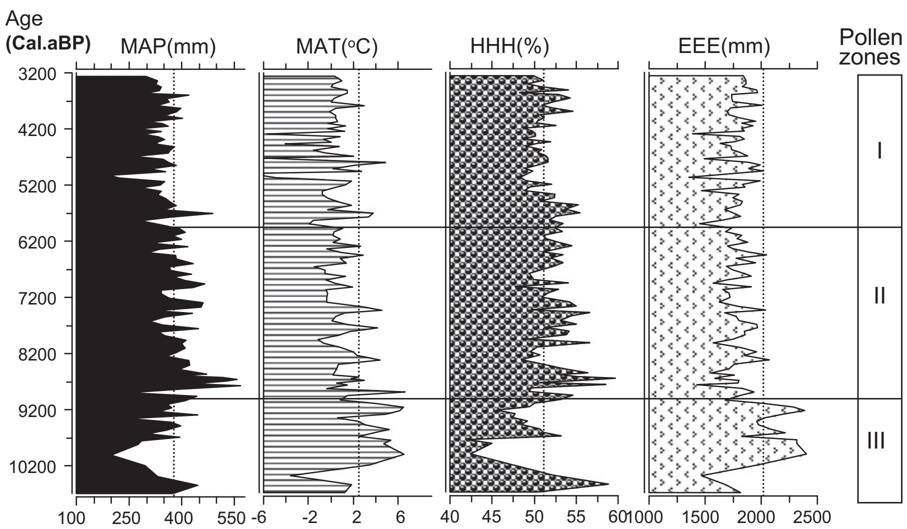

Fig. 11. Time-series of reconstructed mean annual precipitation (MAP), mean annual temperature (MAT), relative humidity (HHH), and annual evaporation (EEE) for the last 10700 cal a BP based on the pollen sequences at the Chen Co Lake, southern Qinghai Tibet Plateau. The vertical dotted line shows the average values of the modern meteorological data at Chen Co Lake region.

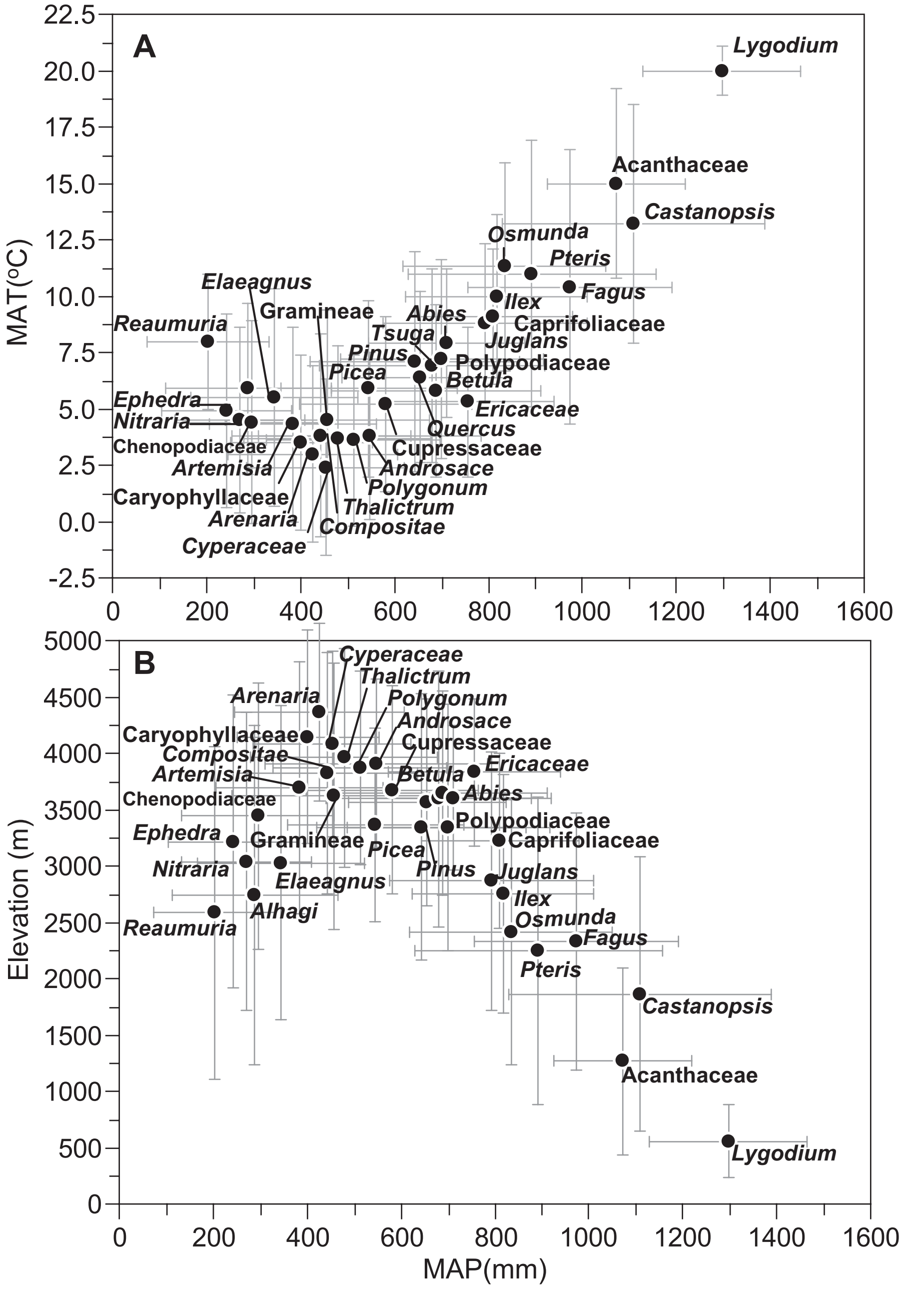

Fig. 12. Optima and tolerances of MAT, MAP and elevation for selected pollen taxa based on weighted averaging. (A) MAT plotted against MAP. (B) Elevation plotted against MAP.

genus level because the differences in pollen morphology among species are too subtle to be distinguished under light microscope. Consequently, the diversity of pollen flora is reduced in comparison with the diversity of plant taxa.

In spite of this, previous studies have successfully established the quantitative relationships between modern pollen rain and climate parameters, and reconstructed palaeo-climatic changes by using typical pollen types (Shen, 2006; Herzschuh et al., 2009a,b, 2010) in the Qinghai-Tibetan Plateau. These examples demonstrate that there is the potential to identify the main vegetation and local climate regions using only the most abundant or significant pollen types.

5.2. Prediction errors

The prediction errors of the pollen-climate transfer functions established here (Table 4) (MAP $_{RMSEP}$ = 109 mm, ca. 5.9% of the MAP range; MAT $_{RMSEP}$ = 2.3 °C, ca. 8.1% of MAT range, etc.) are similar to those of pollen transfer functions developed from 227 modern pollen samples, covering Europe, North Africa, and Siberia (MAP $_{error}$ = 180 mm, MAT $_{error}$ = 2.1 °C)(Guiot et al., 1989), and from 425 modern pollen samples in East Africa (MAP $_{error}$ = 80 mm) (Bonnefille and Chalié, 2000).

Shen (2006) and Herzschuh et al. (2010) documented a smaller estimated error of prediction for MAP (61 mm, 104 mm, respectively) based on the pollen-climate transfer functions developed in some parts of the Qinghai-Tibetan Plateau, but their RMSEP as a percentage of the ranges of MAP is larger (12.4%, 10.6% of the MAP range, respectively). These results suggest that even though our pollen dataset produces a relatively higher RMSEP for the MAP and MAT, our dataset covers a much larger MAP and MAT gradient.

The precision and robustness of our pollen dataset can be further stressed by the fact that we deleted very few sites with larger residual error and no variable (pollen types) as outliers from our dataset compared with similar studies. It is remarkable that the so-called data-screening has been common practice in many studies based on modern pollen, chironomid, or diatom datasets (e.g. Jiang et al., 2001; Lotter et al., 1998; Tarasov et al., 1999).

A number of factors can influence the prediction error of the calibration dataset such as topographical variation resulting in altitudinal temperature and precipitation variations; moreover, human impact on vegetation may be another important factor that complicates many pollen-based climate reconstructions, as suggested by Miehe et al. (2008, 2009a,b). The manner of human driven vegetation change might be an expansion of *Kobresia* meadows at the expense of forests and alpine steppe in the Tibetan Plateau (Miehe et al., 2009a,b). Such information is, however, a basic precondition before considering former population density as a basis for quantifying the probable role and extent of human impact on the vegetation in the vast Tibetan Plateau. In general, the intensity and duration of human impact on vegetation was much higher in the eastern part of China than in the western high mountainous regions (Wu, 1980). For this reason, wherever possible, we selected samples as far as possible away from the area of human activity in the Qinghai-Tibetan Plateau, to ensure that the vegetation composition and hence their pollen assemblages can best reflect their original and natural patterns.

In addition to human impact, the low number of samples and some surface samples with low pollen counts from the western parts of the Qinghai-Tibetan Plateau would increase prediction errors estimated, thus our dataset has to be expanded in the future in order to more accurately reflect the distribution of alpine pollen types in this region.

5.3. Multivariable prediction and corrected altitude

The distributions of pollen in our dataset over the whole Qinghai-Tibetan Plateau are most significantly correlated with MAP. However, in this study we found that changes in the distribution of modern pollen assemblages in surface soils also clearly reflect the MAT, ALT, MT7, HHH, EEE, and CCC, etc. gradients in the CCAs ordination. This suggests that a complicated relationship exists between pollen assemblages and environmental variables in this region.

As reviewed by Seppä et al. (2004), the effect of the environments on plant distribution is rarely controlled by a single environmental variable. Pollen records do probably not only reflect a single climatic parameter (e.g. annual or July mean temperature), but also a variety of other inter-related climatic parameters, including the length of thermal summer and winter, winter minimum temperatures, precipitation and its seasonal distribution, and effective moisture (e.g. Woodward, 1987; Dahl, 1998). Therefore, pollen-based climate reconstructions can offer a wide, coherent insight into the nature of past climates which is increasingly important for interpreting past dynamics of atmospheric circulation patterns (Masson et al., 1999).

However, the use of pollen-climate transfer functions for some palaeo-environmental reconstructions has problems and weaknesses that may limit their usefulness, such as its application as a palaeo-altitude proxy. In fact, the predicted ALT by pollen-climate transfer function represents the altitude of vegetation belts, not the true mountain elevation. Because of climate control, the elevations of vegetation belts in the geological period were generally variable with climatic changes.

Thus, accurate adjustments of climatic influence on the vegetation elevations are needed in order to assess mountain elevation in geological period. Generally, it was thought that the MAT lapse rate can be used to adjust vegetation elevations under different average annual temperatures. But our CCA examination shows that the relationship between the July temperature (MT7) and the vegetation's ALT is completely anti-correlated (Fig. 5A). Thus, we suggest using MT7 to adjust vegetation elevations which shows a better effect than the MAT.

According to the study by Weng and Luo (1990), in the Qinghai-Tibetan Plateau and its surrounding areas, the July temperature (MT7) lapse rate decreases with increasing latitude: $\gamma_{\varphi-7} = 0.7-0.005\varphi$, (Weng and Luo, 1990), in which $\gamma_{\varphi-7}$ = July temperature lapse rate; φ = Latitude (degrees north).

Therefore, a corrected altitude can be calculated by the July temperature, vegetation's ALT, and regional July temperature lapse rate:

$$Y_i = H_i - (\mathrm{MT7_{modern}} - X_i) \times \left(100/\gamma_{\varphi-7}\right), \quad (1)$$

Y_i = corrected altitude (m), $i = 1, \ldots, n$; H_i = calculated altitude (m) (vegetation's ALT) by the transfer function, $i = 1,\ldots, n$; $\mathrm{MT7_{modern}}$ = modern July temperature (°C) in study sites; X_i = calculated July temperature (°C) by transfer functions, $i = 1,\ldots, n$.

The Chen Co Lake is located at latitude of 28.9 °N, therefore the July temperature lapse rate is ca. 0.55 °C/100 m based on Weng and Luo (1990) calculation; or a July temperature change of 1 °C would correspond to an elevation change of 182 m (182 m/1 °C). In the Chen Co Lake region, the modern MT7 is 11.3 °C. Thus:

$$Y_\mathrm{i} = H_i - (11.3 - X_i) \times 182 \quad (2)$$

Fig. 13(A,B) shows the variations in both the vegetation's ALT and the July temperature at Chen Co Lake during the Holocene period. We can see that in the early Holocene the higher July temperature corresponds to a lower vegetation altitude that was predicted by pollen-climate transfer functions. This result suggests that in the early Holocene when the July temperature was higher than the present, the vegetation types found should be in today's relatively low altitude.

During the Holocene, the fluctuation curves of both July temperature and the vegetation's altitude display an obvious mirror image pattern (Fig. 13A,B). The corrected altitude by Formula-2 (Fig. 13C) is close to the present altitude of 4420 m at Chen Co Lake throughout the entire sequence. Since the region's latitude and elevation have not changed since 10,000 cal a BP, we believe that the July temperature lapse rate can be used effectively to calibrate the altitude. Nevertheless, Fig. 13C shows that the corrected altitude curve still has some minor fluctuations, which may be attributed to the influence of other climatic factors.

However, there is still no way to correct accurately a mountain altitude in the past when both altitude and climate changes synchronously affect the pollen records, because it is difficulty to distinguish the effects of altitude from change in the July temperature.

5.4. Understanding thermal-moisture relationship

Temporal patterns of both temperature and precipitation changes in a given region may provide insights into the underlying climate-forcing mechanisms. Earlier works revealed that there was a relatively warm and wet early Holocene and a rather cool and dry late Holocene in the Qinghai-Tibetan Plateau (e.g., Lister et al., 1991; Jarvis, 1993; Van Campo and Gasse, 1993; Kashiwaya et al., 1995; Gasse et al., 1996). However, some lines of evidence suggested that the warmest and wettest period occurred in the middle rather than in the early Holocene in this area (e.g. Shen et al., 1996; Tang et al., 1999). Until now, the importance of these findings has been constrained by difficulties associated with distinguishing temperature and precipitation signals in the sedimentary records. Whether the Asian monsoon intensified gradually or abruptly in response to

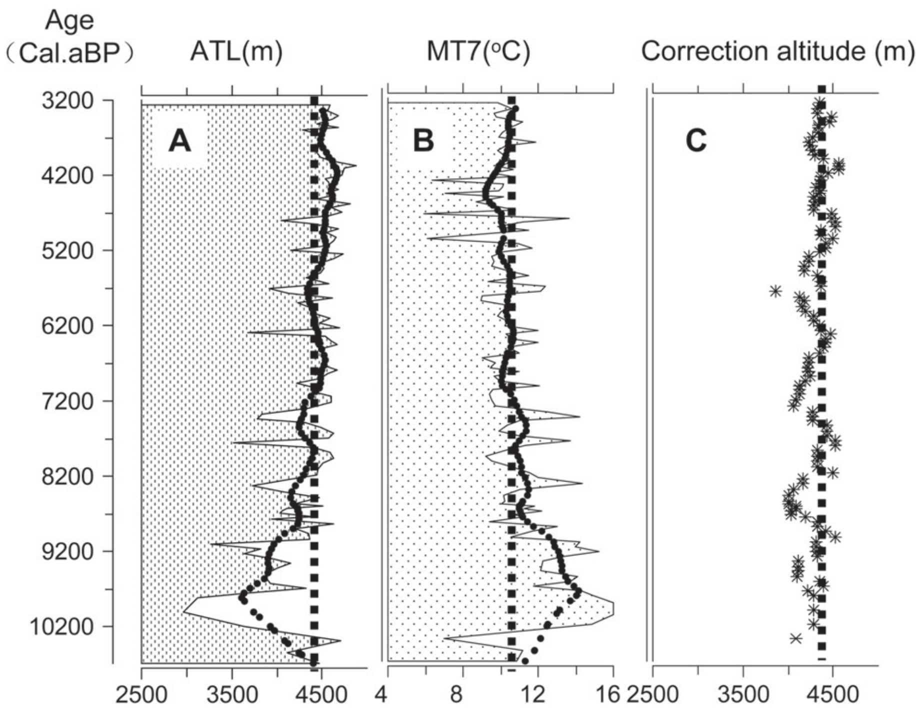

Fig. 13. Corrected altitude at Chen Co Lake region during the last 10,700 cal a BP. (A) Predicted Altitude (ALT) changes by LWWA inference model; (B) Predicted July temperature (MT7) changes by LWWA inference model; (C) Corrected altitude (stars) using July temperature change. The vertical dashed line in A and C shows the modern altitude and that in B shows the modern July temperature at Chen Co Lake region. The black dotted line in A and B is the curve of moving averages. A LOESS smoother (Cleveland, 1979) with a span of 0.1 has been applied to the curves of both ALT and MT7.

increasing insolation remains open to debate (Ruddiman, 2006; Clemens and Prell, 2007).

Our results clearly show that the warmest period occurred between 10,000 and 9000 cal a BP, while the highest precipitation appeared at approximately 9000–6000 cal a BP (Fig. 11).

The early Holocene around Chen Co Lake was characterized by warmer and drier conditions than today; conversely, cooler condition in the middle Holocene was associated with increased regional moisture. These results are similar to previous studies by Zhu et al. (2009) using chemical proxies from Chen Co Lake, that was after 10,500 cal a BP, the climate changed from warm to cold. However, it is difficult for them to distinguish precipitation changes from temperature ones by chemical proxies. Our results suggest that precipitation lag those of temperature changes during the early-middle Holocene in the southern Tibet Plateau. Some other palaeo-climate reconstructions derived from the pollen records in northeastern Qinghai-Tibetan Plateau (Herzschuh et al., 2009a,b) and in northeastern China (Wen et al., 2009), and from mollusk records in the Chinese Loess Plateau (Wu et al., 2002), have also revealed a pattern of climate variations similar to our pollen-based reconstruction.

Our findings are in contradiction with some other palaeo-climate records from monsoon-influenced East Asia, where coupled warmer and wetter climate conditions occurred in the early-middle Holocene (Chen et al., 2008). The so-called Holocene climate optimum period occurred in different times in different regions in Asia. Our study contributes to a better understanding of the regional temperature and precipitation evolution in the southern Qinghai-Tibetan Plateau by highlighting the spatial heterogeneity of past climate changes in individual regions, as suggested by Shen (2003).

5.5. Uncertainty and possible future improvements

The difficulties in reconstructing vegetation and climatic history from palynological records in mountain areas have long been understood (Barthélémy and Jolly, 1989; Cheddadi et al., 1997; Ortu et al., 2006). As reviewed by Seppä et al. (2004) and Ortu et al. (2006), the biases that affect pollen assemblages are mainly resulting from different production, transport, preservation processes, and human impact. For example, both wind-driven uphill transport and water-driven downhill transport are likely to lead to a complex relationship between vegetation and pollen percentages, which may significantly complicate climate inferences.

As mentioned above, in the Qinghai-Tibetan Plateau, there are many unique plant species sharing similar pollen morphological characteristics. This has led to difficulties in distinguishing them, resulting in a lower taxonomic resolution (family or genus level) in palynology. This low taxonomic resolution makes it difficult to precisely pinpoint the inferred climatic conditions associated with critical taxa, and increases the potential for bias in climatic models based on pollen analysis.

Due to all these uncertain factors, pollen-based climate reconstructions are probably not precise enough for reconstructing climatic conditions on annual to seasonal timescales. However, when pollen-stratigraphical studies are carefully designed and implemented they have the potential to provide reliable information about the general, decadal, or centennial to millennial-scale climatic trends, or about major short-term climatic changes that exceed the inherent sample specific errors of the reconstructions (Seppä et al., 2004).

Quantitative reconstructions cannot, therefore, capture the total climatic pattern of the past, especially if the past vegetation and pollen samples have been influenced by a climatic variable not present in the modern calibration set (MacDonald and Edwards, 1991). Thus, more samples are needed to be collected from some regions in the Qinghai-Tibetan Plateau which have not yet been extensively sampled, particularly the driest and coldest parts of the northwest, where no surface or lake samples exist (Fig. 1). Some caution is needed when using these transfer functions for palaeo-climate reconstruction. The different representation of pollen grains in different depositional environments cannot be ignored in palaeo-environmental reconstruction using lake sediment sequences (Yang and Scuderi, 2010).

Generally human transformation creates vegetation types which simulate more arid conditions than really existing in the Qinghai-Tibetan Plateau (Miehe et al., 2006). Combining the transfer function analysis with an integration of human influence would be a new and very promising measure to reduce the noise in pollen-environment relationship.

6. Conclusions

Development of the new transfer functions for multivariable reconstructions of climate conditions from pollen data along significant ecological and climatic gradients over the Qinghai-Tibetan Plateau provides a significant improvement to existing transfer functions within the Qinghai-Tibetan region. It will therefore provide a basis for improved palaeo-climatic reconstructions from Quaternary pollen records in this region. In addition, the analysis of pollen data provides more general insights into the development and application for transfer functions in other parts of the world and perhaps for other microfossils.

Multivariate numerical analyses (DCA and CCA) were used to study the distribution of pollen assemblages from the surface soil samples of 1202 sites in relation to broad eco-climatic conditions in the Qinghai-Tibetan Plateau of China. Of the 13 environmental variables measured, ordination by CCA identified MAP as the most significant variable controlling the distribution and abundance of pollen. MAT, HHH, and ALT etc. also accounted for significant variations in pollen assemblages.

A quantitative transfer function was created to estimate MAP, MT1, MAT, ALT, HHH, EEE, CCC, and MP7 from the surface sedimentary pollen assemblages using locally weighted weighted averaging (LWWA). Significant relationships were established between pollen assemblages and MAP (R^2-boot = 0.89, RMSEP = 109 mm), MAT (R^2-boot = 0.78, RMSEP = 2.3 °C), ALT (R^2-boot = 0.73, RMSEP = 597m), HHH (R^2-boot = 0.82, RMSEP = 4.5%), and MP7 (R^2-boot = 0.87, RMSEP = 23 mm), etc. Our results show highly significant relationships between modern pollen assemblages and major environmental variables, indicating that pollen can provide useful quantitative estimates of past environmental changes in the Chinese Qinghai-Tibetan Plateau.

The transfer functions developed have been tested for a Holocene pollen record in the southern Qinghai-Tibetan Plateau. Our results show that the warmest period occurred at between 10,000 and 9000 cal a BP, and the wettest period (i.e., maximum precipitation) occurred at approximately 9000–6000 cal a BP. Our findings suggest that precipitation changes lag behind temperature changes during the early to middle Holocene in the southern Qinghai-Tibetan Plateau.

We believe that our study provides a more comprehensive understanding of the quantitative relationships between modern pollen rain and climate variables and a more precise reconstruction of past vegetation and climate patterns.

Acknowledgments

We thank Jiaqi Liu, Ping Zhao, Haibin Wu, Jingtai Han, Siwen Bi, Ninglian Wang, Zhaoyan Gu, Yunli Luo, Deke Xu, and Jie Li for their kind help in field sampling, and Suming Wang, Ji Shen, and Wenyin Jiang, Haibin Wu for their valuable suggestions and helpful discussions. We acknowledge Sun Xiangjun, and Luo Yunli for kindly providing Chinese Quaternary Pollen Data Base. Special thanks to Dr. Richard Jones for helpful remarks and language correction. We are also indebted to two anonymous reviewers for their invaluable comments.

This research was supported by the National Science Foundation of China (No. 41071131, 40771216), the National Basic Research Program of China (2005CB422002), and Chinese Academy of Sciences (KZCX2-YW-Q09-03-02; kzcx2-yw-117; 100 Talents Programme).

Appendix. Supplementary material

Supplementary data associated with this article can be found in the online version, at doi:10.1016/j.quascirev.2011.01.008.

References

An, Z., Kutzbach, J.E., Prell, W.L., Porter, S.C., 2001. Evolution of Asian monsoons and phased uplift of the Himalayan–Tibetan plateau since late Miocene times. Nature 411, 62–66.
Barthélémy, L., Jolly, M.C., 1989. Milieux de montagne et palynologie. Acta Biologica Montana 9, 325–332.
Bennion, H., 1994. A diatom-phosphorus transfer function for shallow, eutrophic ponds in southeast England. Hydrobiologia 275/276, 391–410.
Birks, H.J.B., 1995. Quantitative palaeoenvironmental reconstructions. In: Maddy, D., Brew, J.S. (Eds.), Statistical Modelling of Quaternary Science Data. Technical Guide, vol. 5. Quaternary Research Association, Cambridge, pp. 161–254.
Birks, H.J.B., 1998. Numerical tools in quantitative paleolimnology–progress, potentialities, and problems. Journal of Paleolimnology 20, 301–332.
Birks, H.J.B., 2003. Quantitative Palaeoenvironmental Reconstructions from Holocene Biological Data. In: Mackay, A., Battarbee, R.W., Birks, H.J.B., Oldfield, F. (Eds.), Global Change in the Holocene. Arnold, London, pp. 107–123.
Bjune, E., Seppä, H., Birks, H.J.B., 2009. Quantitative summer-temperature reconstructions for the last 2000 years based on pollen-stratigraphical data from northern Fennoscandia. Journal of Paleolimnology 41, 43–56.
Bonnefille, R., Chalié, F., 2000. Pollen-inferred precipitation time series from equatorial mountains, Africa, the last 40 kyr BP. Global and Planetary Change 26, 25–50.
Borcard, D., Legendre, P., Drapeau, P., 1992. Partialling out the spatial component of ecological variation. Ecology 73, 1045–1055.
Brown, K.J., Fitton, R.J., Schoups, G., Allen, G.B., Wahl, K.A., Hebda, R.J., 2006. Holocene precipitation in the coastal temperate rainforest complex of southern British Columbia, Canada. Quaternary Science Reviews 25, 2762–2779.
Chang, D.H.S., 1981. The vegetation zonation of the Tibetan Plateau. Mountain Research and Development 1, 29–49.
Cheddadi, R., Yu, G., Guiot, J., Harrison, S.P., Prentice, I.C., 1997. The climate of Europe 6000 years ago. Climate Dynamics 13, 1–9.
Chen, F.H., Yu, Z.C., Yang, M.L., Ito, E., Wang, S.M., Madsen, D.B., Huang, X.Z., Zhao, Y., Sato, T., Birks, H.J.B., Boomer, I., Chen, J.H., An, C.B., Wünnemann, B., 2008. Holocene moisture evolution in arid central Asia and its out-of-phase relationship with Asian monsoon history. Quaternary Science Reviews 27, 351–364.
Clemens, S.C., Prell, W.L., 2007. The timing of orbital-scale Indian monsoon changes. Quaternary Science Reviews 26, 275–278.
Cleveland, W.S., 1979. Robust locally-weighted regression and smoothing scatter plots. Journal of the American Statistical Association 74, 829–836.
COHMAP Members, 1988. Climatic changes of the last 18,000 years: observation and model simulations. Science 241, 1043–1052.
Cook, E., Kaars, S.V.D., 2006. Development and testing of transfer functions for generating quantitative climatic estimates from Australian pollen data. Journal of Quaternary Science 21, 723–733.
Cour, P., Zheng, Z., Duzer, D., Calleja, M., Yao, Z., 1999. Vegetational and climatic significance of modern pollen rain in northwestern Tibet. Review of Palaeobotany and Palynology 104, 183–204.
Dahl, E., 1998. The Phytogeography of Northern Europe. Cambridge University Press, Cambridge. 297pp.
Fægri, K., Iversen, J., 1975. Textbook of Pollen Analysis. Munksgaard, Copenhagen. 295pp.
Gajewski, K., Lezine, A.M., Vincens, A., Delestan, A., Sawada, M., 2002. Modern climate–vegetation–pollen relations in Africa and adjacent areas. Quaternary Science Reviews 21, 1611–1631.
Gasse, F., Fontes, J.C., Van Campo, E., Wei, K., 1996. Holocene environmental changes in Lake Bangong basin (Western Tibet). Part 4: discussion and conclusion. Palaeogeography, Palaeoclimatology, Palaeoecology 120, 79–92.
Gasse, F., Juggins, S., Ben Khelifa, L., 1995. Diatom-based transfer functions for inferring past hydrochemical characteristics of African lakes. Palaeogeography, Palaeoclimatology, Palaeoecology 117, 31–54.
Gou, X., Chen, F., Jacoby, G., Cook, E., Yang, M., Peng, J., Zhang, Y., 2007. Rapid tree growth with respect to the last 400 years in response to climate warming, northeastern Tibetan Plateau. International Journal of Climatology 27, 1497–1503.
Guiot, J., 1990. Methodology of the last climatic cycle reconstruction in France from pollen data. Palaeogeography, Palaeoclimatology, Palaeoecology 80, 49–69.

Guiot, J., Harrison, S.P., Prentice, I.C., 1993. Reconstruction of Holocene precipitation patterns in Europe using pollen and lake-level data. Quaternary Research 40, 139–149.
Guiot, J., Pons, A., de Beaulieu, J.L., Reille, M., 1989. A 140 000-year climatic reconstruction from two European pollen records. Nature 338, 309–313.
Hall, P., Wilson, S.R., 1991. Two guidelines for bootstrap hypothesis testing. Biometrics 47, 757–762.
Herzschuh, U., Birks, H.J.B., Liu, X.Q., Kubatzki, C., Lohmann, G., 2009a. What caused the mid-Holocene forest decline on the eastern Tibet-Qinghai Plateau? Global Ecology and Biogeography 19, 278–286.
Herzschuh, U., Kramer, A., Mischke, S., Zhang, C.J., 2009b. Quantitative climate and vegetation trends since the late glacial on the northeastern Tibetan Plateau deduced from KouchaLake pollen spectra. Quaternary Research 71, 162–171.
Herzschuh, U., Birks, H.J.B., Mischke, S., Zhang, C., Böhner, J., 2010. A modern pollen-climate calibration set based on lake sediments from the Tibetan Plateau and its application to a Late Quaternary pollen record from the Qilian Mountains. Journal of Biogeography 37, 752–766.
Holmgren, B., Tjus, M., 1996. Summer air temperatures and tree line dynamics at Abisko. Ecological Bulletin 45, 159–165.
Huang, C.X., Van Campo, E., Doublemei, F., 1993. A study on pollen in surface soil from the western Xizang. Arid Land Geography 16, 75–83 (in Chinese with English abstract).
Imbrie, J., Kipp, N.G., 1971. A new micropaleontological method for Quantitative Paleoclimatology: application to a late pleistocene caribbean Core. In: Turekian, K.K. (Ed.), The Late Cenozoic Glacial Ages. Yale University Press, New Haven, CT, pp. 71–181.
Institute of Geography, 1990. Map of the Qinghai-Tibetan Plateau. Science Press, Beijing (in Chinese)102–112.
Institute of Geography, 1999. The National Physical Atlas of China. China Cartographic Publishing House, Beijing, 230 pp.
ITCAS (Investigation Team of ChineseAcademy of Science), 1988. Vegetation in Tibetan Plateau. Science Press, Beijing (in Chinese), 497pp.
Jarvis, D.I., 1993. Pollen evidence of changing Holocene monsoon climate in Sichuan Province, China. Quaternary Research 39, 325–337.
Jiang, H., Seidenkrantz, M.-S., Knudsena, K.L., Eirýksson, J., 2001. Diatom surface sediment assemblages around Iceland and their relationships to oceanic environmental variables. Marine Micropaleontology 41, 73–96.
Jiang, W., Guiot, J., Chu, G., Wu, H., Yuan, B., Hatté, C., Guo, Z., 2010. An improved methodology of the modern analogs technique for palaeoclimate reconstruction in arid and semi-arid regions. Boreas 39, 145–153.
Jongman, R.H.G., ter Braak, C.J.F., van Tongeren, O.F.R., 1995. Data Analysis in Community and Landscape Ecology. Cambridge University Press, Cambridge, 324 pp.
Juggins, S., 2001. The European Diatom Database, User Guide. University of Newcastle. http://craticula.ncl.ac.uk/Eddi/docs/EddiGuide.pdf, 72 pp.
Juggins, S., 2003. User Guide: C2, Software for Ecological and Palaeoecological Data Analysis and Visualization User Guide Version 1.3. Department of Geography University of Newcastle, Newcastle upon Tyne, 69 pp.
Kashiwaya, K., Masuzawa, T., Morinaga, H., Yaskawa, K., Yuan, B., Liu, J., Gu, Z., 1995. Changes in hydrological conditions in the central Qing-Zang (Tibetan) Plateau inferred from lake bottom sediments. Earth and Planetary Science Letters 135, 31–39.
Kutzbach, J.E., Guetter, P.J., Ruddiman, W.F., Prell, W.L., 1989. The sensitivity of climate to late Cenozoic uplift in southern Asia and the American west: numerical experiments. Journal of Geophysical Research 94, 18393–18407.
Li, Y.C., Xu, Q.H., Liu, J.S., Yang, X.L., Nakagawa, T., 2007. A transfer-function model developed from an extensive surface-pollen data set in northern China and its potential for palaeoclimate reconstructions. The Holocene 17, 897–905.
Lin, Z.H., Mo, X.G., Li, H.X., Li, H.B., 2002. Comparison of three spatial interpolation methods for climate variables in China. Acta Geographica Sinica 57 (1), 47–56 (in Chinese with English abstract).
Lister, G.S., Kelts, K., Chen, K., Yu, J., Niessen, F., 1991. Lake Qinghai, China: closed-basin lake levels and the oxygen isotope record for Ostracoda since the latest Pleistocene. Palaeogeography, Palaeoclimatology, Palaeoecology 84, 141–162.
Liu, H.Y., Cui, H.T., Pott, R., Speier, M., 1999. The surface pollen of the woodland-steppe ecotone in southeastern Inner Mongolia, China. Review of Palaeobotany and Palynology 105, 237–250.
Liu, K.-b., Lam, N.S.N., 1985. Paleovegetational reconstruction based on modern and fossil pollen data: an application of discriminant analysis. Annals of the Association of American Geographers 75, 115–130.
Liu, T.C., 1995. Changes of Yamzhuo Lake water levels in Xizang. Scientia Geographica Sinica 15, 55–62 (in Chinese with English abstract).
Liu, X.D., Chen, B., 2000. Climatic warming in the Tibetan Plateau during recent decades. International Journal of Climatology 20, 1729–1742.
Lotter, A.F., Birks, H.J.B., Holfgang, W., Marchetto, A., 1998. Modern diatom, cladocera, chironomid, and chrysophyte cyst assemblages as quantitative indicators for the reconstruction of past environmental conditions in the Alps. II. Nutrients. Journal of Paleolimnology 19, 443–463.
Lu, H.Y., Wu, N.Q., Liu, K.-B., Jiang, H., Liu, T.S., 2007. Phytoliths as quantitative indicators for the reconstruction of past environmental conditions in China II: palaeoenvironmental reconstruction in the Loess Plateau. Quaternary Science Reviews 26, 759–772.
Lu, H.Y., Wu, N.Q., Yang, X.D., Jiang, H., Liu, K.B., Liu, T.S., 2006. Phytoliths as quantitative indicators for the reconstruction of past environmental conditions in China I: phytolith-based transfer function. Quaternary Science Reviews 25, 945–959.
Lu, H.Y., Wu, N.Q., Yang, X.D., Shen, C.M., Zhu, L.P., Wang, L., Li, Q., Xu, D.K., Tong, G.B., Sun, X.J., 2008. Spatial pattern of Abies and Picea pollen distribution along the elevation gradient in the Qinghai–Tibetan plateau and Xinjiang, China. Boreas 37, 254–262.
MacDonald, G.M., Edwards, K.J., 1991. Holocene palynology: I principles, population and community ecology, palaeoclimatology. Progress in Physical Geography 15, 261–289.
Masson, V., Cheddadi, R., Braconnot, P., Joussaume, S., Texier, D., PMIP participants, 1999. Mid-holocene climate in Europe: what can we infer from PMIP model-data comparisons? Climate Dynamics 15, 163–182.
Members of China Quaternary Pollen Data Base, 2001. Simulation of China Biome reconstruction based on pollen data from surface sediment samples. Acta Botanica Sinica 43, 201–209.
Miehe, G., Miehe, S., Schlütz, F., Kaiser, K., Duo, L., 2006. Palaeoecological and experimental evidence of former forests and woodlands in the treeless desert pastures of Southern Tibet (Lhasa, A.R. Xizang, China). Palaeogeography, Palaeoclimatology, Palaeoecology 242, 54–67.
Miehe, G., Miehe, S., Will, M., Opgenoorth, L., Duo, L., 2008. An inventory of forest relicts in the pastures of Southern Tibet (Xizang A.R., China). Plant Ecology 194, 157–177.
Miehe, G., Miehe, S., Kaiser, K., Reudenbach, C., Behrendes, L., Duo, L., Schlütz, F., 2009a. How old is pastoralism in Tibet? An ecological to the making of a Tibetan landscape. Palaeogeography, Palaeoclimatology, Palaeoecology 276, 130–147.
Miehe, G., Miehe, S., Schlütz, F., 2009b. Early human impact in the forest ecotone of southern High Asia (Hindu Kush, Himalaya). Quaternary Research 71, 255–265.
Nakagawa, T., Tarasov, P.E., Nishida, K., Gotanda, K., Yasuda, Y., 2002. Quantitative pollen-based climate reconstruction in central Japan: application to surface and Late Quaternary spectra. Quaternary Science Reviews 21, 2099–2113.
Ortu, E., Brewer, S., Peyron, O., 2006. Pollen-inferred palaeoclimate reconstructions in mountain areas: problems and perspectives. Journal of Quaternary Science 21, 615–627.
Overpeck, J.T., Webb III, T., Prentice, I.C., 1985. Quantitative interpretation of fossil pollen spectra: Dissimilarity coefficients and the method of modern analogs. Quaternary Research 23, 87–108.
Rioual, P., Andrieu-Ponel, V., de Beaulieu, J.L., Reille, M., Svobodova, H., Battarbee, R.W., 2007. Diatom responses to limnological and climatic changes at Ribains Maar (French Massif central) during the Eemian and early Würm. Quaternary Science Reviews 26, 1557–1609.
Ruddiman, W.F., 2006. What is the timing of orbital-scale monsoon changes? Quaternary Science Reviews 25, 657–658.
Seppä, H., Birks, H.J.B., Odland, A., Poska, A., Veski, S., 2004. A modern pollen–climate calibration set from northern Europe: developing and testing a tool for palaeoclimatological reconstructions. Journal of Biogeography 31, 251–267.
Seppä, H., Bjune, A.E., Telford, R.J., Birks, H.J.B., Veski, S., 2009. Last nine-thousand years of temperature variability in Northern Europe. Climate of the Past 5, 523–535.
Shao, X.M., Huang, L., Liu, H.B., Liang, E.Y., Fang, X.Q., Wang, L.L., 2005. Reconstruction of precipitation variation from tree rings in recent 1000 years in Delingha, Qinghai. Science in China (Series D) 48, 939–949.
Shen, C.M., 2003. Millennial-scale variations and centennial-scale events in the southwest Asian monsoon: pollen evidence from Tibet. PhD thesis, Louisiana State University and Agricultural and Mechanical College, USA, 286 pp.
Shen, C.M., Liu, K.-B., Tang, L.Y., Overpeck, J.T., 2006. Quantitative relationships between modern pollen rain and climate in the Tibetan Plateau. Review of Palaeobotany and Palynology 140, 61–77.
Shen, C.M., Tang, L.Y., Wang, S., 1996. Vegetation and climate during the last 22,000 years in Zoige region. Acta Micropalaeontologica Sinica 13, 401–406 (In Chinese with English abstract).
Shen, C.M., Liu, K.-B., Tang, L.Y., Overpeck, J.T., 2008. Numerical analyses of modern and fossil pollen data from the Tibetan Plateau. Annals of the Association of American Geographers 98, 755–772.
Solovieva, N., Tarasov, P.E., Donald, G.M., 2005. Quantitative reconstruction of holocene climate from the Chuna Lake pollen record, Kola Peninsula, northwest Russia. The Holocene 15, 141–148.
Song, C.Q., Lu, H.Y., Sun, X.J., 1997. Boreal pollen–climatic factor transfer function and its application in paleoclimate reconstruction. Chinese Science Bulletin 42, 2182–2186 (in Chinese).
South China Institute of Botany & Institute of Botany, Academia Sinica, 1982. Angiosperm Pollen Flora of Tropic and Subtropic China. Science Press, Beijing (in Chinese), 452 pp+219 plates.
Sun, X.J., Wang, F.Y., Song, C.Q., 1996. Pollen–climate response surfaces of selected taxa from Northern China. Science in China (D) 39, 486–493.
Tang, L., Shen, C., Liu, K., Overpeck, J.T., 1999. New high-resolution pollen records from two lakes in Xizang (Tibet). Acta Botanica Sinica 41, 896–902.
Tarasov, P., Granoszewski, W., Bezrukova, E., Brewer, S., Nita, M., Abzaeva, A., Oberhänsli, H., 2005. Quantitative reconstruction of the last interglacial vegetation and climate based on the pollen record from Lake Baikal, Russia. Climate Dynamics 25, 625–637.
Tarasov, P.E., Peyron, O., Guiot, J., Brewer, S., Volkova, V.S., Bezusko, L.G., Dorofeyuk, N.I., Kvavadze, E.V., Osipova, I.M., Panova, N.K., 1999. Last glacial maximum climate of the formed Soviet Union and Mongolia reconstructed from pollen and plant macrofossil data. Climate Dynamics 15, 227–240.

ter Braak, C.J.F., 1986. Canonical correspondance analysis: a new eigenvector technique for multivariate direct gradient analysis. Ecology 67, 1167–1179.
ter Braak, C.J.F., 1988. Canoco–a FORTRAN program for canonical community ordination by (partial) (detrended) (canonical) correspondence analysis, principal components analysis and redundancy analysis (version 2.1). Technical Rep. LWA-88-02. GLW, Wageningen, 95 pp.
ter Braak, C.J.F., 1994. Canonical community ordination. Part I: basic theory and linear methods. Ecoscience 1, 127–140.
ter Braak, C.J.F., Juggins, S., 1993. Weighted averaging partial least squares regression (WA-PLS): an improved method for reconstructing environmental variables from species assemblages. Hydrobiologia 269/270, 485–502.
ter Braak, C.J.F., Prentice, I.C., 1988. A theory of gradient analysis. Advances in Ecological Research 18, 271–317.
ter Braak, C.J.F., Smilauer, P., 2002. CANOCO 4.5. Biometris. Wageningen University and ResearchCenter, Wageningen, 500 pp.
ter Braak, C.J.F., Verdonschot, P.F.M., 1995. Canonical correspondence analysis and related multivariate methods in aquatic ecology. Aquatic Sciences 57, 255–289.
Van Campo, E., Gasse, F., 1993. Pollen- and diatom-inferred climatic and hydrological changes in the Sumxi Co Basin (western Tibet) since 13,000 yr B.P. Quaternary Research 39, 300–313.
Wang, F.H., Chien, N.F., Zhang, Y.L., Yang, H.Q., 1995. Pollen Flora of China, Second Edition. Science Press, Beijing (in Chinese) 461 pp+205 plates.
Wang, J.T., 1988. The steppes and deserts of the Xizang plateau (Tibet). Vegetation 75, 135–142 (in Chinese).
Weckström, J., Korhola, A., Blom, T., 1997. The relationship between diatoms and water temperature in thirty subarctic Fennoscandian lakes. Arctic and Alpine Research 29, 75–92.
Wen, R.L., Xiao, J.L., Chang, Z.G., Zhai, D.Y., Xu, Q.H., Li, Y.C., Itoh, S., 2009. Holocene precipitation and temperature variations in the East Asian monsoonal margin from pollen data from Hulun Lake in northeastern Inner Mongolia, China. Boreas. doi:10.1111/j.1502-3885.2009.00125.x 0300–9483.
Weng, D.M., Luo, Z.X., 1990. Mountainous Topography Climate. Meteorological Press, Beijing (in Chinese) 541 pp.
Whitmore, J., Gajewski, K., Sawada, M., Williams, J.W., Minckley, T., Shuman, B., Bartlein, P.J., Webb III, T., Viau, A.E., Shafer, S., Anderson, P., Brubaker, L.B., 2005. A north American modern pollen database for Multi-scale Paleoecological and Paleoclimatic Applications. Quaternary Science Reviews 24, 1828–1848.
Woodward, F.I., 1987. Climate and Plant Distribution. Cambridge University Press, Cambridge, 174 pp.
Wu, N.Q., Liu, T.S., Liu, X.P., Gu, Z.Y., 2002. Mollusk record of millennial climate variability in the Loess plateau during the last glacial maximum. Boreas 31, 20–27.
Wu, Y.S., Xiao, J.Y., 1995. A preliminary study on modern pollen rain of Zabuye salt lake area, Xizang. Acta Botanica Yunnaica 17, 72–78 (in Chinese with English abstract).
Wu, Z., 1980. Vegetation of China. Science Press, Beijing (in Chinese), 1275 pp.
Yan, S., Kong, Z.C., Yang, Z.J., Zhang, Y., Ni, J., 2004. Seeking relationship between vegetation and Picea pollen in surface soil of Xinjing, northwestern China. Acta Ecologica Sinica 24, 2017–2023 (in Chinese with English abstract).
Yang, X., Kamenik, C., Schmidt, R., Wang, S., 2003. Diatom-based conductivity and water-level inference models from eastern Tibetan (Qinghai-Xizang) Plateau lakes. Journal of Paleolimnology 30, 1–19.
Yang, X.P., Scuderi, L.A., 2010. Hydrological and climatic changes in deserts of China since the late Pleistocene. Quaternary Research 73, 1–9.
Yao, T., Duan, K., Xu, B., Wang, N., Guo, X., Yang, X., 2008. Precipitation record since AD 1600 from ice cores on the central Tibetan Plateau. Climate of the Past 4, 175–180.
Yu, G., Tang, L.Y., Yang, X.D., Ke, X.K., Hassisong, S.P., 2001. Modern pollen samples from alpine vegetation on the Tibetan Plateau. Global Ecology and Biogeography 10, 503–519.
Zhang, Y.L., Xi, Y.Z., Zhang, J.T., Gao, G.Z., Du, N.Q., Sun, X.J., Kong, Z.C., 1990. Spore Morphology of Chinese Pteridophytes. Science Press, Beijing, China (in Chinese) 364 pp+91plates.
Zhang, E.L., Jones, R., Bedford, A., Langdon, P., Tang, H.G., 2007. A Chironomid-based salinity inference model from lakes on the Tibetan Plateau. Journal of Paleolimnology 38, 477–491.
Zheng, Z., Huang, K.Y., Xu, Q.H., Lu, H.Y., Cheddadi, R., Luo, Y.L., Beaudouin, C., Luo, C.X., Zheng, Y.W., Li, C.H., Wei, J.H., Du, C.B., 2008. Comparison of climatic threshold of geographical distribution between dominant plants and surface pollen in China. Science in China Series (D) 51, 1107–1120.
Zhu, L.P., Zhen, X.L., Wang, J.B., Lu, H.Y., Xie, M.P., Kitagawa, H., Göran Possnert, G., 2009. A ~30,000-year record of environmental changes inferred from Lake Chen Co, Southern Tibet. Journal of Paleolimnology 42, 343–358.
Zhao, Y., Herzschuh, U., 2009. Modern pollen representation of source vegetation in the QaidamBasin and surrounding mountains, northeastern Tibetan Plateau. Vegetation History and Archaeobotany 18, 245–260.
Zhao, Y., Xu, Q.H., Huang, X.Z., Guo, X.L., Tao, S.C., 2009. Difference of modern pollen assemblages from lake sediments and surface soils in arid and semi-arid China and their significance for pollen–based quantitative climate reconstruction. Review of Palaeobotany and Palynology 156, 519–524.